Abstract

This thesis addresses the problem of letting two mobile telephone customers use the same frequency and/or time slot simultaneously. It presents an algorithm, which performs multivariable equalizing and detection, using a multivariable Decision Feedback Equalizer (DFE). The DFE presented can be used for arbitrary numbers of receivers and transmitters.

This algorithm is utilized on two different multivariable channel models, one deterministic and one stochastic. These models map characteristics of the antenna system onto channel characteristics. In the deterministic model, the phase difference of the carrier wave at the two antennas is the parameter, and for the stochastic model the envelope correlation of the signals at the two antennas is used. Monte Carlo simulations have been carried out on a simple FIR channel from a purely discrete-time viewpoint.

The results obtained from the deterministic model are very good, but rest on specific assumptions. The stochastic model also produces good results. Although it potentially can double the system capacity, already for moderately correlated antennas, the algorithm produces a BER, which is lower than a single antenna configuration succeeds with. A comparison has also been made with conventional antenna diversity methods, and also with a multivariable DFE with two antennas and one message. For the latter case, the achieved BER is superior for any antenna correlation.

Acknowledgements

I am most grateful to my supervisors Dr Anders Ahlén and Dr Mikael Sternad. I would also like to express my gratitude to Lars Lindbom for enlightening and stimulating discussions.

Contents

Chapter 1

Introduction

In the ancient times, personal communications meant talking. The people taking part in the conversation could be at most a few tens of meters apart. The need for communications over larger distances was enormous, and soon after man had become settled, the written word was invented. Writing remained the main communication method for long distances over a very long period of time, and it is only recently it has received serious competition as the most important way of communicating over long distances.

The written word has three major drawbacks however. First of all, it is slow. Writing is a slow process, and delivering letters takes far too long time. Secondly, writing has never been, and will never be, as easy as talking. Thirdly, and probably most important, writing is not interactive. Even today, it takes a few minutes or more for the reply of an electronic letter to reach the original sender.

At the time of the industrial revolution, the demand for better communications was enormous. During the 18th century, the *optical telegraph* was massively utilized in France. A system of *semaphores* covered entire France. Its successor, the *electric telegraph*, became the next step in the development of personal communications. Actually, these methods were not "personal" at all. They both relied on operators delivering the message, letter by letter. Hence, the contents of the messages were no secrets.

It was not until the end of the 19th century that two inventions changed the business of long-distance personal communications. First, Alexander Graham Bell invented the telephone. This made it feasible, if not easy, to communicate interactively over long distances (across continents). This communication was basically private. Two persons were given unique access to a communication channel, and although it was possible for others to intercept their communication, it required some effort.

To name the telephone system the ultimate "personal communication" system would be to say too much, however. The wire or cable based telephone system is very stationary, and when you call a person, you do not really call the person. Rather, you direct your call to a specific location where the person in question is supposed to be. This would be in contrast to the situation where the great

invention of the early 20th century was used, the *wireless radio*.

The italian Marconi used radio waves to transmit messages. The message needed no medium to travel in. The invention was also called wireless. This gave a possibility for truly personal communication. If you brought your wireless radio transmitter and receiver with you wherever you went, you would always be reachable. Unfortunately, the communication would not be private. Anyone with a radio of the same kind could easily listen to the conversation.

Through the years, the wireless radios became smaller and smaller. Finally, in the 1950's, it was time for the arrival of the *mobile telephone system*. This system combined the advantages of the telephone and the wireless radio. To start with, these systems were analogue, but later on they became digital. The development today indicates that very soon, the majority of new telephone (and data) connections installed, will be radio connections.

The digital mobile telephone systems produce a vast of technological challenges. There is a general demand to accommodate as many users as possible within some given limits. Another important issue is to guard against disturbances and weak signals, something that is common in these systems. One solution to this problem has been to use multiple antennas to reduce the impact of noise. The main idea with this approach is that the receiving conditions will almost surely not be the same at all the antennas simultaneously. Multiple antennas can also be used to solve more fundamental problems, such as e.g. capacity limitation. This issue is investigated in this thesis.

Assuming that there are two antennas at each base station and two antennas[1] *at each mobile, is it possible for two users to use the same frequency simultaneously, by using the information from their two receiver antennas in a clever way?*

This naturally leads to the problem of multivariable channel models, and how the channel models are related to measurable properties of the antenna system. Two multivariable channel models are presented in this thesis, one deterministic and one stochastic. The stochastic is the most promising one. The major parameter in this model is the envelope correlation of the two signals arriving to (or arriving from) the two base station antennas.

The next problem to consider is how to construct a multivariable filter, which extracts the transmitted information from distorted and noisy measurements. The multivariable channel is supposed to be exactly known and time invariant. We decide to use a multivariable *Decision Feedback Equalizer* (DFE) after having considered both a multivariable *Linear Feedback Equalizer* (LFE) and a multivariable *Viterbi detector*. The design equations for a multivariable DFE, which are derived, can, in principle, be used for an arbitrary number of transmitters and receivers. The design equations are logical generalizations of those for the scalar case, derived

[1] The methods presented in this thesis can be generalized to multiple antennas, but we restrict ourselves to two.

by Sternad and Ahén in [16] and used by e.g. Lindbom in [12]. The multivariable filter design equations constitute a linear system of equations, $\mathbf{AX=B}$, where $\mathbf{X}$ and $\mathbf{B}$ are *matrices*, not vectors. The special case when there is a single transmitter and multiple receivers is very similar to the maximal ratio combiner discussed in [5].

This work fits really nice into the future development of mobile radio systems. Today, digital mobile telephone systems based on three different standards (GSM [2], ADC[3], JDC[4]) are in operation or under development. But future systems are already being considered. There is no doubt that these systems will operate at higher carrier frequencies than today's systems. This will simplify the design of handheld units with multiple antennas, since the necessary spacing between different antennas is closely related to the carrier wavelength. There are several fundamental design issues for these future systems that are discussed. One point where the discussion is particularly fierce is the choice of multiplexing method. The method presented in this thesis can be used whichever of FDMA [5], TDMA [6] or CDMA [7] is finally decided for. However, the use of CDMA would in itself decrease the correlation among the antennas, which would be very beneficial in the present case.

The thesis is organized as follows: chapter 2 contains a brief overview of digital radio and mobile communications. Chapter 3 presents the multivariable channel models that will be used. Chapter 4 presents the filters and equalizers that will be used. In chapter 5, a Monte Carlo simulation study is presented, together with a comparison with today's methods. Finally, in chapter 6 the thesis is summarized and some conclusions are drawn.

[2]GSM=Global System for Mobile communication
[3]ADC=American Digital Cellular
[4]JDC=Japanese Digital Cellular
[5]FDMA=Frequency Division Multiple Access, each user gets a private frequency
[6]TDMA=Time Division Multiple Access, each user gets a private time slot
[7]CDMA=Code Division Multiple Access, each user gets a private code

Chapter 2

Mobile radio communication

2.1 Digital radio communication

2.1.1 The radio transmission system

Figure 2.1: The radio system.

A radio transmission system basically consists of three parts. At one end is the transmitter. The transmitter accepts information from a source, transforms it into a form that can be transmitted and sends it over a *Radio Frequency* (RF) channel. The channel possibly distorts the transmitted signal before it reaches the receiver. It is then the receivers job to figure out what signal was transmitted, and to turn it into understandable information. If everything goes well, the information the receiver delivers should coincide with the information fed into the transmitter.

Digital communication differ from its analogue counterpart in that it can only transmit a finite number of waveforms. The information is typically a stream of binary digits. These binary digits could either be converted analogue signals, or they can be purely digital. They might in the latter case originate from a computer.

The information reaching the transmitter is typically coded, i.e. it has already been processed. In the same way, the information that leaves the receiver must be decoded before it can be used. Neither encoding nor decoding will be discussed further in this thesis. Moreover, the treatment of digital communication systems in general is very brief in this thesis. For a complete treatment of such systems, see [13].

2.1.2 The transmitter

In the transmitter, the bit stream is first divided into groups of k bits. Each group is combined into a *symbol*. A symbol is the smallest unit of information that is transmitted over a radio channel. Instead of a stream of bits, a stream of symbols

is transmitted. The total set of symbols is referred to as an *alphabet*.

Symbols can not be transmitted as they stand, since they are digital. Through *pulse shaping*, the digital symbols are converted into analogue waveforms. The pulse shaping is basically accomplished through low pass filtering, where some constraints are put on the low pass filter. This technique is called *Pulse Amplitude Modulation* (PAM), and the signal is called a PAM signal.

After the pulse shaping, the PAM signal is referred to as the *baseband* signal. The next step in the signal conditioning process is *modulation*. Modulation means that the baseband signal $s_b(t)$ is multiplied by a continuous time sine or cosine function of high frequency (ω_c), the so-called *carrier*,

$$s_p(t) = s_b(t)\cos(\omega_c t) \ .$$

The resulting signal $s_p(t)$ is called the *passband* signal. In the case of mobile telephone communications, the carrier frequency lies in the *microwave range*. This means that the wavelength is between 0.3 m and 0.001 m, and the frequency between 900 MHz and 300 GHz. The microwave region is also called the UHF (Ultra High Frequency) region. The effect the modulation has on the baseband signal is that it shifts it to a much higher frequency, see Figure 2.2.

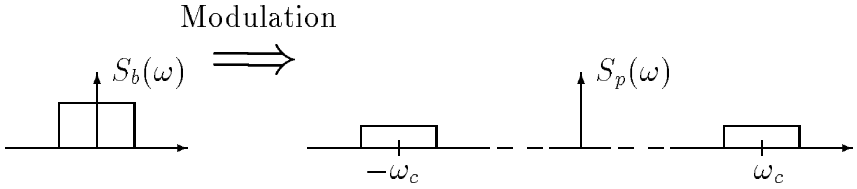

Figure 2.2: Baseband and passband spectrum for a real valued signal, which has been modulated by a carrier $\cos\omega_c t$.

The spectrum of the baseband signal is *symmetrical*, if the signal is *real-valued*. This property would be insignificant if the baseband signal was to be transmitted itself, since the part of the spectrum that has a negative frequency is not really transmitted. However, when the passband signal is studied, the situation is different. The part of the spectrum that lies below the carrier frequency (the lower sideband) is also transmitted and occupies frequency space without providing any additional information. One way of avoiding this drawback and to transmit additional information in the lower sideband, is to allow the symbols to be complex-valued. It is of course impossible to transmit a complex-valued signal as it stands, because the real world in general, and the RF channel in particular, is not complex-valued. The solution is to multiply the possibly complex baseband signal with a complex carrier and transmit the real part of the corresponding signal:

$$s_p(t) = \mathrm{Re}\{s_b(t)e^{j\omega_c t}\} \ .$$

This is, in fact, equivalent to transmitting the real and imaginary parts of the pulse shaped symbol $s_b = s_b^r + js_b^i$ separately, using two carriers that have the same frequency but phases that differ by 90 degrees.

For complex-valued symbols, the baseband spectrum is not symmetrical around $\omega = 0$, and the corresponding passband spectrum is not symmetrical around $\omega = \omega_c$. Hence this modulation scheme uses the frequency space more efficiently.

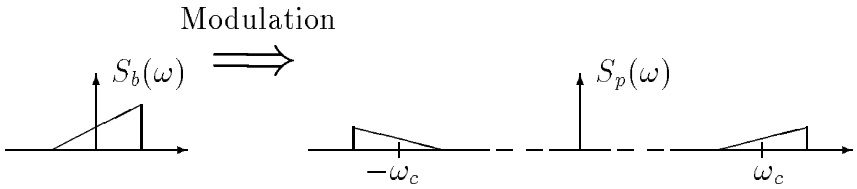

Figure 2.3: Baseband and passband spectrum for complex-valued signals, modulated by a complex carrier $e^{j\omega_c t}$.

Two modulation techniques that use complex symbols, and which are commonly used in practise, are QAM (*Quadrature Amplitude Modulation*) and PSK (*Phase Shift Keying*). In QAM, the symbols are transmitted as described above. Multiplying the pulse-shaped signal with a complex carrier $e^{-j\omega_c t}$ and transmitting the real part is equivalent to splitting the baseband signal $s_b(t)$ into real and imaginary parts, modulating them separately by $\cos\omega_c t$ and $-\sin\omega_c t$ and transmitting the sum, see Figure 2.4. The signal $s_b^r(t)\cos\omega_c t$ is denoted the *in-phase* component while the signal $-s_b^i(t)\sin\omega_c t$ is denoted the *quadrature* component.

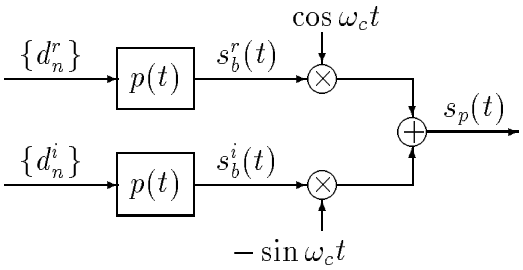

Figure 2.4: A QAM transmitter. $p(t)$ is the pulse shaping filter.

In PSK, the complex-valued symbols are restricted to have the same amplitude, i.e. $\{d_n\} = \{re^{j\theta_n}\}$. After the modulation, the entire information is conveyed by the phase of the modulated carrier. It is clear that QAM and PSK are closely related, since

$$\mathrm{Re}\{d_n\} = r\cos\theta_n \qquad \mathrm{Im}\{d\}_n = r\sin\theta_n \ .$$

2.1.3 The channel

It is not quite clear what is meant by an RF (Radio Frequency) channel. The type of channel description depends on the purpose. Some people may only want to consider the space between the transmitting and receiving antenna as the channel. The channel is then continuous in time. It is also possible to consider the channel to be discrete in time. In that case, the modulation at the transmitter and demodulation, prefiltering and sampling at the receiver are included in the channel,

as well as the wave propagation properties of the space between the transmitting and receiving antenna. This second view is adopted in this thesis. The discrete channel models used in this thesis will have the transmitted symbols $d(k)$ as inputs and the received sampled baseband signals $y(k)$ as outputs.

The by far most crucial aspect of the discrete-time channel, which complicates the receiver design, is the "free" space between antennas. The quotation marks are well justified; only on very rare occasions may this space be considered free from obstacles. In fact, objects around and between the transmitter and the receiver reflect and scatter the radio waves as they travel through the ether.

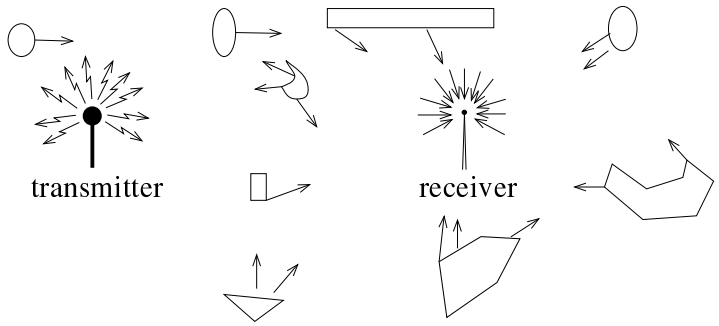

Figure 2.5: The mobile radio environment. A very large number of scatterers contribute to multipath propagation.

As the obstacles are located at different distances from the transmitter and receiver, the same signal will reach the receiver at different time instants. This leads to a *delay spread*. The delay spread may cause the same signal to arrive at the receiver at different sampling instants. The received signal at one time instant may consist of, not only of the latest symbol transmitted, but also of symbols transmitted in the preceding sampling instants. This effect is called *intersymbol interference* (ISI). The channel can then be considered as a linear difference equation, with the symbols $d(k)$ as input and the received sampled baseband signals $y(k)$ as outputs:

$$y(k) = b_0 d(k) + b_1 d(k-1) + b_2 d(k-2) + \ldots + b_n d(k-n) + v(k) \; . \qquad (2.1)$$

The signal $v(k)$ comprises *noise* and interference, and describes the part of $y(k)$ which can not be modelled as a linear regression of the symbols $d(k)$. The existence of a bandpass filter in the receiver assures that $v(k)$ has zero mean. Apart from that, the distribution and spectral characteristics of $v(k)$ are unknown. In the above model, the sampling interval is normalized to $T = 1$, and k here denotes *discrete* time. The frequency response of the channel will in general not be flat. The channel is then called *frequency-selective*, since some frequencies are attenuated more than other. Using the backward shift operator q^{-1} ($q^{-1}y(k) = y(k-1)$), the *impulse response* (or *transfer operator*) $B(q^{-1})$ of the channel can be written

$$B(q^{-1}) = b_0 + b_1 q^{-1} + b_2 q^{-2} + \ldots + b_n q^{-n} \; . \qquad (2.2)$$

The coefficients (also known as *taps*) of (2.2) are in general complex, even for real-valued symbols $d(k)$. At first glance, this might seem strange, but is a consequence

of the baseband representation of a passband channel. Consider transmission of real-valued PAM signals. The baseband and passband representation of the *transmitted* signal is shown in Figure 2.2. The RF channel can be represented by its *continuous-time, passband* impulse response $h(t)$ or its corresponding transfer function $H(j\omega)$, shown in Figure 2.6.

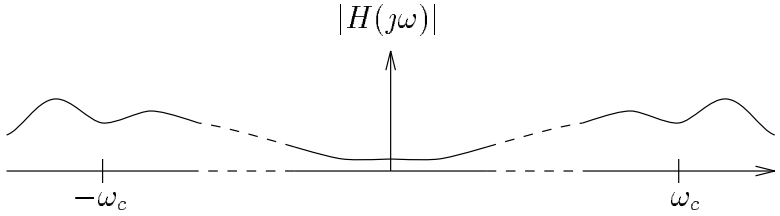

Figure 2.6: The continuous-time, passband transfer function of a RF channel.

To obtain the spectrum of the *received* passband signal $r_p(t)$, the transfer function $H(j\omega)$ is multiplied by the transmitted signal spectrum $S_p(\omega)$, shown in Figure 2.2. This results in a received passband spectrum shown in Figure 2.7. Also shown in Figure 2.7 is the spectrum, which the received baseband signal $r_b(t)$ has after the demodulation.

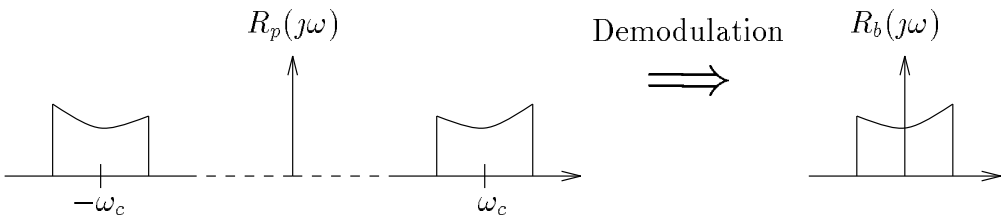

Figure 2.7: The demodulation process. Notice that the resulting baseband spectrum $R_b(j\omega)$ is not symmetrical with respect to $\omega = 0$, even though the passband spectrum $R_p(j\omega)$ is.

The resulting baseband spectrum of the received signal is not symmetrical with respect to $\omega = 0$. We want to describe the entire process from Figure 2.2 to Figure 2.7 with only one transfer function $H_b(j\omega)$ from one baseband signal to another. We do not want to take the modulation and demodulation explicitly into account every time the channel is considered. This is possible, but this transfer function must have an asymmetrical spectrum. But only complex-valued functions have asymmetrical spectra. Hence, our equivalent baseband impulse response (2.2), which is the inverse Fourier transform of $H_b(j\omega)$, must be complex-valued. This is the price that has to be paid in order to be able to make (almost) all considerations in the baseband.

The conclusion of the argument above is that the equivalent baseband impulse response of the passband transmission is given by (2.2): a polynomial with complex coefficients. These coefficients might well be time-variant, but throughout this thesis, they are supposed to be time-invariant.

The performance of a well-designed radio system primarily depends on the channel. It is interesting to measure the quality of the channel. The usual way to do this is by using the *Signal-to-Noise Ratio* (SNR). The SNR in discrete time is defined as

$$\text{SNR} \triangleq \frac{E[|u(k)|^2]}{E[|v(k)|^2]} \tag{2.3}$$

where $v(k)$ is defined as in (2.1) and

$$u(k) = B(q^{-1})d(k) \ .$$

The relationship between this definition and the SNR discussed in continuous time, the signal–to–noise ratio per bit E_b/N_0, is affected by many things. The relationship depends among other things on the receiver prefilter and the size of the symbol alphabet.

2.1.4 The receiver

In the receiver, the received signal is demodulated. This is accomplished by multiplying the signal by $\cos \omega_c t$ and $-\sin \omega_c t$, respectively. The respective components are then passed through a low-pass prefilter and sampled. The sampled quadrature component is multiplied by $\jmath$ and finally the two components are added, to produce the received (complex-valued) baseband signal $y(kT)$.

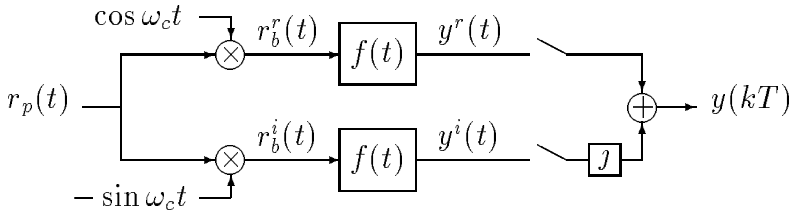

Figure 2.8: The QAM receiver, where $r_p(t)$ is the received passband signal and ω_c is the carrier frequency. The in-phase and quadrature components are demodulated and sampled separately. Notice that here k denotes the time index. In the following chapters, the time index used will be t. T is the sampling interval.

The problem is now to reconstruct the initial symbols from these measurements. Note that the effect of the pulse shaping filter $p(t)$ and the receiver filter $f(t)$ on the received signal $y(k)$ will, in the following, be included in the total baseband channel model (2.1).

The performance of a digital radio system is often measured in how many percent of the symbols or bits were not detected correctly. These figures should be as small as possible. In this thesis, the size of the alphabet is two (binary signalling). Hence, the two measures are the same, but the unit *Bit Error Rate* (BER), is the one that will be used.

2.2 The mobile radio environment

2.2.1 The cellular radio system

Mobile telephone systems are basically built around a large number of *base stations*. An antenna is associated with each base station. This antenna is often situated well above the terrain surrounding it. Each base station provides telephone services to a number of *mobiles*. A mobile can be a vehicle based telephone or a hand-held terminal. Each mobile is given unique access to one channel by the base station. This is in contrast to e.g. walkie-talkies.

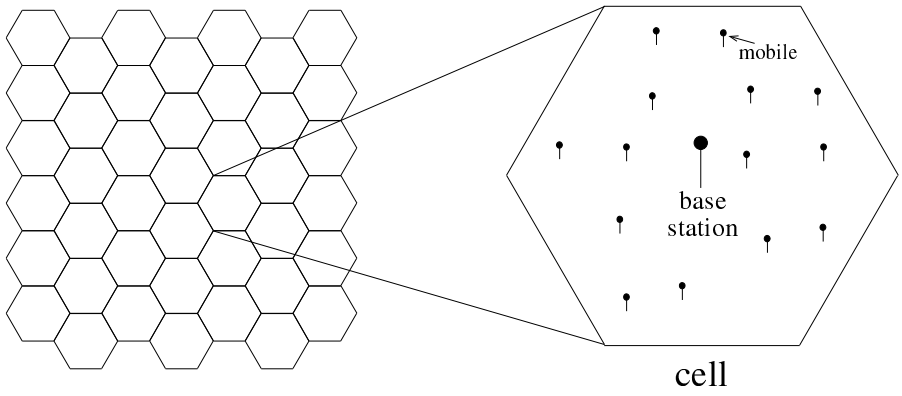

Figure 2.9: The cellular system, used in a mobile telecommunication system. The real pattern of the cells is actually much more irregular and complicated than the simple hexagonal one sketched in the figure.

All mobiles served by one base station are said to be in the same *cell*. A cell is of course a limited geographical region. However, it is not necessary (or common) for a base station to be in the middle of its cell. The border between two adjacent cells are not well defined. The selection of the particular base station which communicates with a certain mobile and the *handover* (switching) of a mobile from one base station to an adjacent one, is handled dynamically from case to case by a higher order control system. This system continuously monitors the received signals' strengths from the different mobiles.

Except for containing the antenna and analogue amplifiers, a base station quite naturally provides some administrative services to its mobiles. The most important of these services is, of course, (at least today) the connection to the usual, stationary telephone system. Other services provided by the higher order, supervisory system includes channel management, i.e. the system decides which channel is allocated to which mobile. This can be solved in many ways, depending on how the available frequencies are divided among the mobiles. Methods such as FDMA, TDMA and CDMA are possible ways to split the frequency band. Multiplexing methods will, however, not be discussed in this thesis. An overview of the area can be found in e.g. [3]. Also, in most systems used today, the entire frequency band can not be used by a single base station. The base station must coordinate its channel usage with that of the neighboring base stations'. Despite this

coordination, the major reason for noise in cellular radio systems is *co-channel interference*, i.e. the "noise" a mobile in one cell is experiencing mostly stems from other mobiles in other cells, using the same channel. The typical cell radius is 1-30 km. The size of a cell is dictated by the number of expected subscribers in the area. The means of regulating the cell size is the transmitter power, antenna height and the geographical and topographical locations of the base stations. One possibility to increase capacity in such a system is to increase the number of base stations, and decrease their range (the size of the cells).

The carrier frequency used for mobile communication is very high, typically in the lower microwave region. The microwave region corresponds to a frequency of about 900 MHz to 300 GHz, and a wavelength between 0.3 m and 1 mm. Presently, frequencies in bands around 450 MHz, 900 MHz and 1.8 GHz are allocated for mobile telephony in Europe. Experiments are carried out for the use of considerably higher frequencies. These frequencies are intended for use in in-door picocells and wide-band digital systems.

2.2.2 Multipath fading

In mobile communication, one part of the radio link is generally moving. Thus communication is to be established between a fixed base station and a mobile in motion. The radio link from the mobile to the base station is called the *uplink*, and the reversed link is called the *downlink*. As a result of the motion, the channel will be time varying. Since the channel is varying, also the received signal strength will vary. This phenomenon is called *fading*.

There are basically two types of fading: *long-term* fading and *short-term* fading. Long-term fading occurs when the mobile is obscured by large objects, such as e.g. a mountain or a forest. This fading is rather slow: once behind the mountain, the channel will not change much until the mobile leaves the vicinity of the mountain. This typically takes many minutes.

Short-term fading, on the other hand, is not caused by single objects. The collective effect of many small objects (typically houses or trees in an urban or suburban environment) causes locally reflected waves to produce a stationary interference pattern. The channel at one location can be quite different from the channel one meter away, and if the mobile is moving, the channel might change completely within milliseconds; hence the name short-term fading. Since this effect stems from the fact that the signals travel many different ways to the mobile (multipath propagation), short-term fading is also known as *multipath fading*. For a comprehensive discussion of multipath fading, see e.g. [11], [12].

Fading is most often discussed in terms of temporal variation, but it is actually more appropriate to discuss it in terms of spatial variation. This is because it is a *spatial* change the mobile experiences as it travels through the interference pattern; the pattern itself is stationary, as long as the majority of the scatterers are stationary.

2.2.3 Rayleigh fading

The delay spread that causes the channel to have an impulse response which lasts over several sampling intervals, is not the only effect caused by multipath propagation. It is in fact very likely that multipath propagation exists, even when there is no intersymbol interference. This effect causes each channel coefficient in (2.2) to be a sum of many locally reflected waves, with small differences in travelling times. Each of them is associated with a damping factor $a_i^{(k)}(x)$ and a phase shift $\psi_i^{(k)}(x)$, which are both spatially varying:

$$b_k(x) = \sum_{i=1}^{N_k} a_i^{(k)}(x) e^{j\psi_i^{(k)}(x)} \qquad k = 0, 1, \ldots, n \ .$$

A commonly accepted model for the distribution of the coefficients is the *Rayleigh fading* model (see [9]). This model describes the channel coefficients as mutually independent, complex Gaussian variables, i.e.

$$b_k^r(x) \triangleq \mathrm{Re}\{b_k\} \in \mathcal{N}(0, \sigma_k) \qquad b_k^i(x) \triangleq \mathrm{Im}\{b_k\} \in \mathcal{N}(0, \sigma_k) \ .$$

$$E[b_k^r(x) b_k^i(x)] = 0 \ .$$

The spatial variation can be expressed in terms of the normalized covariance function of the coefficients. The normalized covariance function is defined as:

$$R(\xi) \triangleq \frac{E[b_k^p(x) b_k^p(x-\xi)]}{E[b_k^p(x)]^2} \qquad p = r, i \ . \tag{2.4}$$

where ξ is the distance between two points along the direction x. In a Rayleigh fading environment, $R(\xi)$ is given by a Bessel function of the first kind and of order zero:

$$R(\xi) = J_0(2\pi \frac{\xi}{\lambda}) \ . \tag{2.5}$$

The above properties are based on the following assumptions:

- The mobile is reached by an infinite number of locally reflected waves ($N_k \to \infty$).
- The surrounding local scatterers are symmetrically distributed around the mobile.
- The coefficients $a_i(x)$ are considered to be independent, identically distributed, random variables, with average power independent of i.
- All the phases are mutually independent random variables, with uniform distributions on $[0, 2\pi]$.

This model has been verified to be accurate (see [9]) under the conditions

1. The receiver antenna is located close to the ground
2. The carrier wavelength is small enough (<0.3m).

In an urban or suburban environment, these assumptions apply very well to the situation around the mobile, *but they do not apply to the situation around the base station.* This is because there are few, if any, local scatterers surrounding the base station. Hence, only a small number of locally reflected waves reach the base station antennas, which violates assumption 1 above for Rayleigh fading. As a matter of fact, there is no well-accepted model which describes the fading at the base station.

The Rayleigh fading model does not say anything about the correlation between *different* taps in the channel model. The view adopted in this thesis is that the taps in the channel are mutually uncorrelated. The pulse shaping filter $p(t)$ and the prefilter $f(t)$ most likely introduce some correlation among the taps. This is ignored in this thesis, however.

A fading model closely related to the Rayleigh fading model, is the so-called *Rice fading model.* In this model, one incoming ray is supposed to be stronger than the other ones. This leads to different properties of the channel coefficients, compared to the properties in the Rayleigh fading model. The single, stronger ray is supposed to originate from a direct wave, not locally scattered. This model is also a commonly used one, however not as common as the Rayleigh fading model.

2.2.4 Antenna diversity

The major problem with mobile radio communications is the uncertain channels. There is no way to guarantee a good channel, since the channel is basically stochastic. The Rayleigh fading model makes the randomness of the channel quite obvious. When all the channel coefficients are small, the SNR of the channel becomes very low (cf (2.3)). This situation is referred to as a *fading dip.*

One way to reduce this problem at the base station would be to establish another channel to the mobile. This method is known as *antenna diversity*, and each channel that can be established is referred to as a *branch.* It is then possible to simply use the best branch, or even better, combine the branches in some way. Antenna diversity can be accomplished in many ways, depending on how the other channels are established. One method uses multiple antennas to get different channels. This is called *spatial diversity.* An overview of antenna diversity and different combining methods can be found in [3].

The four most common ways to combine the signals from two antennas are:

1. Selection diversity.
2. Maximal ratio combining.
3. Equal gain combining.
4. Switched diversity.

Selection diversity simply selects the strongest signal and feeds it into the receiver.

Maximal ratio combining is the most powerful but also the most complex method. For a single-tap channel, each signal is weighted by the conjugate of its channel coefficient. (This is in fact the optimal combiner for the AWGN channel.) In the case the phase shift of the channel is not known (non–coherent detection), the branches are weighted by the envelopes of their respective signals. Then the weighted signals are added and fed into the receiver.

Equal gain combining just adds the signals and feeds the sum into the receiver.

Finally, switched diversity uses one signal as long as its signal power is above a certain threshold, but as soon is goes beneath it, the reception is switched to another branch. Compared to selection diversity, this reduces the number of switching transients. This is the simplest method.

If the two branches are assumed to be uncorrelated, the three first methods improve the average SNR in the following way, cf [3]:

- selection diversity: 1.8 dB.
- maximal ratio combining: 3 dB.
- equal gain combining: 2.5 dB.

The improvement that is accomplished using switched diversity, is smaller than that of selection diversity.

The problem with the first two methods is that with today's equipment, the SNR must be estimated in continuous time. However, if the signal from each branch were demodulated, prefiltered and sampled separately, the channel to each antenna could easily be estimated. The SNR is then trivial to calculate.

This is all very fine and dandy. But the critical point is whether the channels can be considered independent. This is clearly a function of the distance between the antennas. If the problem is to obtain uncorrelated channels in a Rayleigh fading environment, the required distance would be around half a carrier wavelength, i.e. around 0.15 m at 900 MHz. However, at the base station, the situation is different. At the base station, it is much more difficult to guarantee uncorrelated signals, since the Rayleigh fading model is not usually applicable there.

2.2.5 Multiple antennas - a possibility to increase capacity?

When there exist two receiver antennas, and the signal from each branch is demodulated, prefiltered and sampled separately, the relation (2.1) can be written

$$\begin{pmatrix} y_1(k) \\ y_2(k) \end{pmatrix} = \begin{pmatrix} b_{01}(x) \\ b_{02}(x) \end{pmatrix} d(k) + \begin{pmatrix} b_{11}(x) \\ b_{12}(x) \end{pmatrix} d(k-1) + \ldots + \begin{pmatrix} b_{n1}(x) \\ b_{n2}(x) \end{pmatrix} d(k-n) + \begin{pmatrix} v_1(k) \\ v_2(k) \end{pmatrix}. \tag{2.6}$$

Both $y_i(k)$ and $v_i(k)$, $i = 1, 2$ are actually functions of x, but for simplicity, this dependence is not written out explicitly in this thesis. Consider a case where there

is only one tap in each channel, and the noise is negligible. Equation (2.6) then becomes

$$\begin{pmatrix} y_1(k) \\ y_2(k) \end{pmatrix} = \begin{pmatrix} b_{01}(x) \\ b_{02}(x) \end{pmatrix} d(k) \ .$$

This can be considered as a overdetermined linear system of equations, which is solved for $d(k)$ in some sense. But there is another interesting possibility: what if another message is added? Then the channel model would look like this:

$$\begin{pmatrix} y_1(k) \\ y_2(k) \end{pmatrix} = \begin{pmatrix} b^1_{01}(x) & b^2_{01}(x) \\ b^1_{02}(x) & b^2_{02}(x) \end{pmatrix} \begin{pmatrix} d_1(k) \\ d_2(k) \end{pmatrix} \ . \tag{2.7}$$

This situation would represent an attempt to transmit two messages simultaneously, and hence potentially double the capacity of the system. If the matrix in (2.7) is non-singular, the system (2.7) would be solvable. A solvable system should imply a good possibility to filter out the desired signals, and vice versa: with a singular or badly conditioned matrix, a large risk of error can be expected. Of course, when more taps are present in the channel and noise is present in the system, the problem becomes more complicated. However, even then, the problem is a "simple" multivariable filtering problem.

The question is now how well a system with two receiver antennas and two messages could perform? It is evident, that a good starting point for the analysis would be to examine the matrix in (2.7). The elements of the matrix are stochastic variables with some distributions. Is it possible to guarantee that this matrix is non-singular? In general, this is not possible. However, it is more likely that a matrix with random elements is non-singular than singular. So, if the elements are uncorrelated, the matrix will probably be non-singular. But if the elements *are* correlated, the matrix might very well be singular. As an extreme example, consider the case when the columns are perfectly correlated, while the rows are completely uncorrelated. This is the case when the paths from $d_1(k)$ and $d_2(k)$ to $y_i(k)$ $i = 1, 2$ are identical, due to a very small separation between the two transmitters. The model is then reduced to

$$\begin{pmatrix} y_1(k) \\ y_2(k) \end{pmatrix} = \begin{pmatrix} b^1_{01}(x) & b^1_{01}(x) \\ b^1_{02}(x) & b^1_{02}(x) \end{pmatrix} \begin{pmatrix} d_1(k) \\ d_2(k) \end{pmatrix} \ .$$

The matrix is clearly singular. When the columns become less correlated, the matrix becomes better conditioned, and the probability of transmission error decreases. This is the main subject of this thesis: how will the probability of error (and hence the BER) be affected by the correlation between the signals?

Chapter 3

Multivariable channel models

As pointed out in the preceding chapter, the key issue for how well a multi-antenna multi-mobile-system would work is the principal appearance of the matrix in (2.7). It would be nice to be able to build a deterministic model, which describes the situation well. Such a model may, for instance, predict the BER as a function of the difference of the incoming angle of the two rays from the mobiles. However, such a model is often hard to obtain. In that case, it is necessary to apply a stochastic model instead. Such models can typically be based on less restrictive assumptions. However, only statistical properties of the channel can be used for prediction of performance.

3.1 Remarks on the notation

From now on, continuous time will not be discussed. Therefore, t denotes *discrete* time, and the sampling interval is normalized to $T = 1$.

In this thesis, all signals are assumed to be complex, if not stated otherwise. Constant matrices are denoted by boldface roman letters, such as $\mathbf{P}$. The transpose of a complex matrix is denoted $\mathbf{P}^T$, and means only transposition of the matrix, not complex conjugation of its elements.

The expression $\overline{\mathbf{P}}$ on the other hand, means that all elements in the matrix $\mathbf{P}$ are complex conjugated, but remain in their places. Finally, $\mathbf{P}^*$ means that $\mathbf{P}$ is transposed and that all its elements are complex conjugated.

For polynomials, the following notation is used: scalar polynomials are denoted by capital, italic and light letters. For any scalar polynomial $P(q^{-1}) = p_0 + p_1 q^{-1} + \ldots + p_{n_p} q^{-n_p}$, define the *conjugate polynomial*

$$P_*(q) = p_0^* + p_1^* q + \ldots + p_{n_p}^* q^{n_p} \ .$$

Matrix polynomials will be denoted by boldface script symbols, like $\boldsymbol{B}(q^{-1})$. (The same convention applies for polynomial matrices, but those will not be used in this thesis.) Similar to the scalar case, the definition for the related conjugate polynomial $\boldsymbol{B}_*(q)$ is

$$\boldsymbol{B}_*(q) = \mathbf{B}_0^* + \mathbf{B}_1^* q + \ldots + \mathbf{B}_{n_b}^* q^{n_b} \ .$$

When appropriate, the backward and forward shift operators are often substituted by the complex transform variables z^{-1} and z respectively.

Finally, rational functions of polynomials, i.e. transfer operators or transfer functions, are denoted by capital, calligraphic letters, e.g. $\mathcal{C}(q^{-1})$ or $\mathcal{C}(z^{-1})$.

3.2 A deterministic model

As a matter of fact, a deterministic channel model can be found only for the uplink, if at all. The model below model assumes a *very* clean environment around the base station. Any reflexes, which reach the receiver within one sampling interval are supposed to arrive from almost the same angle, in other words the model assumes there exist no local reflexes. The difference between the distances the waves have travelled is considered so small, that the power of the signals (i.e. the magnitude of the channel coefficients) are the same for both branches. There will only be a difference in the carrier phase between the two channels, and this is modelled by a multiplication of a complex number of magnitude one. Figure 3.1 shows the geometry of the problem.

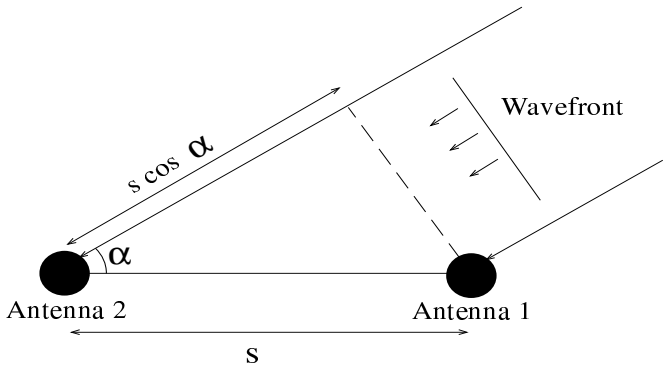

Figure 3.1: Geometry for deterministic channel model.

It is now assumed that the rays from the two mobiles arrive from angles α_1 and α_2 relative to the baseline of length s between the antennas. The matrix in (2.7) is then given by:

$$\mathbf{B} = \begin{pmatrix} b_1 & b_2 \\ b_1 e^{-\jmath\varphi_1} & b_2 e^{-\jmath\varphi_2} \end{pmatrix} \tag{3.1}$$

where the phase φ_i of the ith mobile is related to the incident angle α_i of the ray from the same mobile by

$$\varphi_i = \frac{2\pi s}{\lambda} \cos \alpha_i \qquad i = 1, 2 \ .$$

The complete deterministic model then looks like this:

$$\begin{aligned} \underline{y}(t) &= \begin{pmatrix} y_1(t) \\ y_2(t) \end{pmatrix} = \\ &= \mathbf{B}_0 \begin{pmatrix} d_1(t) \\ d_2(t) \end{pmatrix} + \mathbf{B}_1 \begin{pmatrix} d_1(t-1) \\ d_2(t-1) \end{pmatrix} + \ldots + \mathbf{B}_n \begin{pmatrix} d_1(t-n) \\ d_2(t-n) \end{pmatrix} + \begin{pmatrix} v_1(t) \\ v_2(t) \end{pmatrix} \end{aligned} \tag{3.2}$$

where

$$\mathbf{B}_k = \begin{pmatrix} b_{1k} & b_{2k} \\ b_{1k}e^{-\jmath\varphi_{1k}} & b_{2k}e^{-\jmath\varphi_{2k}} \end{pmatrix} . \tag{3.3}$$

The theoretical calculations as well as the simulation study will be devoted to the single tap case. When that problem is studied in detail, it is revealed (see Appendix B) that only the phase *difference*

$$\Delta\varphi = \varphi_2 - \varphi_1$$

effects the probability of error, i.e. it is possible to set $\varphi_1 = 0$ without any restriction. This is equivalent to turning the antenna system so that the baseline between the antennas is perpendicular to the incoming beam from the mobile corresponding to the first column of (3.1).

Ideally, this model can be used for any antenna spacing. A large antenna separation would make it possible to resolve closely located mobiles, since a small difference in incoming angle would result in a large phase difference $\Delta\varphi$. On the other hand, *widely* separated mobiles could in this case be hard to separate, since different incoming angles will result in the same phase difference. For instance, $s = 10\lambda$ would result in a phase difference $\Delta\varphi = \pi$ for an angular separation of only three degrees, but a phase difference $\Delta\varphi = 2\pi$ for six degrees. The former would be very advantageous, but the latter disastrous. However, when the assumption of no local reflexes is violated (which it probably is), the magnitude of the signals can not be assumed to be the same at the two antennas, and it is not probable that the two phases are so well determined either. For the model to be robust (give a reasonable description even when the assumptions are not quite fulfilled), it is thus necessary to use a rather small spacing between the antennas, maybe half a carrier wavelength. For larger spacings, local reflexes will probably make the deterministic model useless. However, a too small separation would result in a too small phase difference, so the necessary compromise is a delicate one.

It is important to note, that this model is only applicable to the uplink case. This is because ignoring local reflexes at the mobile would be an extremely bad approximation. If there were two antennas at the mobile (which is assumed later in this thesis), the channel to these two antennas would be quite random, even if they were placed less than half a carrier wavelength apart. There would not exist any deterministic phase difference, assuring that the matrix (3.1) is not badly conditioned.

3.3 A stochastic model

3.3.1 The downlink

Since a deterministic model has been proposed for the uplink, it is natural to first consider the downlink in the stochastic case. The general idea is to *transmit two different messages from the two base station antennas.* Two assumptions are made concerning the mobile, the first of which is:

- There are two antennas at the mobile.

This assumption is presently valid in the Japanese Digital Cellular (JDC) mobile radio system. The next assumption is the following:

- The mobile is in a Rayleigh fading environment, with the antennas separated by at least half a carrier wavelength.

A schematic picture of the spatial variation of two Rayleigh faded taps is shown in Figure 3.2.

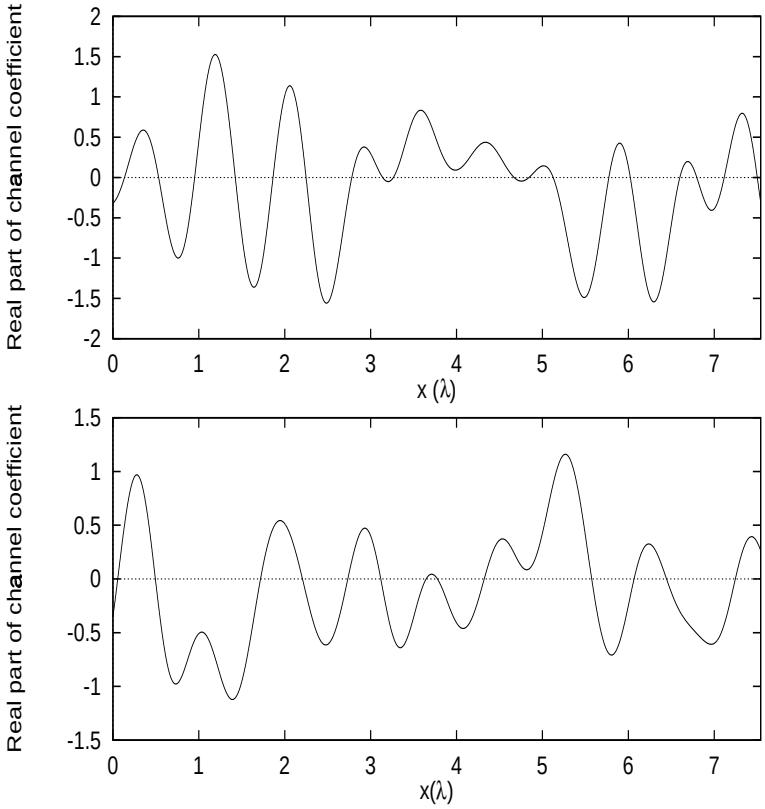

Figure 3.2: Real part of two channel coefficients in a Rayleigh fading environment. The upper figure shows $b_{01}^1(x)$, i.e. the channel from base station antenna 1 to mobile 1, while the lower shows $b_{01}^2(x)$, i.e. the channel from base station antenna 2 to mobile 1. The correlation between the two channel coefficients is a critical parameter in the thesis. Note that the position x is given in the unit of carrier wavelengths.

The last assumption assures that the two channels are uncorrelated. The validity of this assumption can surely be argued about. It can, however, easily be accomplished if the mobile is a car telephone. A separation of half a wavelength is less than half a meter in the microwave range, while a car is at least 1.5 meters wide. On a hand-held terminal, this separation is much more difficult to accomplish. However, in future systems, the carrier frequency will be higher, and the carrier wavelength will decrease accordingly. For a carrier frequency of 1.8 GHz presently allocated for mobile telephony in Europe, the carrier wavelength will 15 cm, and

hence the necessary separation will be smaller. In either case, the correlation between the two received signals may still be significant, and the consequences of this are interesting subjects for further studies.

No assumption is made on the correlation between the signals arriving from the two base station antennas. This correlation is allowed to vary and it is a major parameter in this thesis. Considering the single-tap case only, the matrix in (2.7) is now described by

$$\mathbf{B}_0(x) = \begin{pmatrix} b_{01}^1(x) & b_{01}^2(x) \\ b_{02}^1(x) & b_{02}^2(x) \end{pmatrix} \tag{3.4}$$

where the elements in (3.4) are stochastic variables, having the following second order moments:

$$E[|b_{0k}^m(x)|^2] = \text{SNR} \qquad k,m = 1,2 \tag{3.5}$$

$$E[b_{01}^k(x) b_{02}^k(x)] = 0 \qquad k = 1,2 \tag{3.6}$$

$$\frac{E[b_{01}^{1r}(x) b_{01}^{2r}(x)]}{E[b_{01}^{1r}(x)^2]} = J_0(2\pi \frac{s}{\lambda})$$

$$\frac{E[b_{01}^{1i}(x) b_{01}^{2i}(x)]}{E[b_{01}^{1i}(x)^2]} = J_0(2\pi \frac{s}{\lambda})$$

where s is the antenna separation. The definition of the SNR stems from the fact that both the signals $\{d(t)\}$ and the noise have unit variance. Actually, it would be appropriate to define an SNR for each antenna, but throughout this thesis, the signals received and transmitted at the antennas are considered to have equal average power.

However, the BER will not be studied as a function of the correlation of the channel coefficients themselves. Instead, it is studied as a function of the correlation of the *envelopes* of the signals, primarily because these are easier to measure. The major parameter in the thesis is thus the *envelope correlation*

$$\rho_d \triangleq \frac{E[|b_{01}^1(x)||b_{01}^2(x)|] - E[|b_{01}^1(x)|]E[|b_{01}^2(x)|]}{E[|b_{01}^1(x)|^2] - (E[|b_{01}^1(x)|])^2} \ . \tag{3.7}$$

Notice that the columns are elementwise correlated, while the rows are elementwise uncorrelated. Equations (3.4)–(3.7) constitute the stochastic model for the downlink investigations. When the channel consists of more than one tap, all taps have all but one of the above properties. The taps have identical distributions, and are mutually uncorrelated. The only difference is the definition of SNR. In this case, (3.5) becomes

$$E[\sum_{l=0}^{n} |b_{lk}^m(x)|^2] = \text{SNR} \qquad k,m = 1,2 \ . \tag{3.8}$$

3.3.2 The uplink

If the deterministic model of Section 3.2 can not be applied, due to the existence of significant multipath propagation, it would be nice to be able to use a stochastic model in the uplink as well. The assumption that must be made is in this case

- The signals from the two transmitters (mobiles) have uncorrelated channels.

It is easily realized, that the only difference between the stochastic downlink model and the stochastic uplink model will be the correlations between the elements in (3.4). In the stochastic uplink model, the columns are elementwise uncorrelated, while the rows are elementwise correlated. This is reciprocal to the uplink case. The relations (3.4)–(3.7) are then modified to

$$E[|b_{0k}^{m}(x)|^2] = \mathrm{SNR} \qquad k, m = 1, 2$$

$$E[b_{0k}^{1}(x) b_{0k}^{2}(x)] = 0 \qquad k = 1, 2$$

$$\rho_u \triangleq \frac{E[|b_{01}^{1}(x)||b_{02}^{1}(x)|] - E[|b_{01}^{1}(x)|]E[|b_{02}^{1}(x)|]}{E[|b_{01}^{1}(x)|^2] - (E[|b_{01}^{1}(x)|])^2} \,. \tag{3.9}$$

For a thorough calculation of the correlation at the base station antenna, see [9].

It is worth noting, that the two uncorrelated transmitter antennas can be at the *same* mobile if a Rayleigh fading environment is assumed, as well as on two separate mobiles. This makes it possible to increase *speech quality* when the traffic load in the system is low, thus using the free system capacity. One way to improve quality is to split the stream of bits, which are to be transmitted, into two separate streams. Each bit stream is transformed into a stream of symbols, and transmitted from a separate antenna. This can be done both in the uplink and in the downlink. The free capacity can then be used to allow more elaborate coding techniques to achieve lower resulting BER, or it can be used simply to transmit more data, if the reliability of the radio link is good enough.

3.4 The utilization of the channel models

In Chapter 5, the above models are used as a basis to conduct Monte Carlo simulations. With a channel assumed *exactly known*, an *equalizer* is optimized. This equalizer is used on the simulated data, and the number of errors encountered are counted. The ratio between the number of errors and the number of data is an estimate of the BER.

The models that will be simulated are the following:

- The deterministic model is simulated for a single-tap channel as a function of $\Delta\varphi$ with SNR as a parameter. For SNR=0dB, the simulation results will be compared with a theoretical calculation.
- The stochastic model is simulated for a single-tap channel and a two-tap channel, both in the uplink and downlink. The results are obtained as a function of the envelope correlation (3.7) and (3.9), with SNR as a parameter.

Before discussing the outcome of these simulations any further, some candidates for multivariable equalizer structures must first be derived.

Chapter 4

Equalizers

The equalizer is the part of the receiver, which tries to remove the noise and distortion from the received signals. In the present thesis, the equalizer operates completely in discrete time. The equalizers commonly used operates on sequences of data, which are scalars. This case is studies in the first part of this chapter. In the second part of the chapter, the focus is moved to equalizers which operates on multiple data (i.e. vectors) simultaneously. These are referred to as *multivariable equalizers*, in contrast to the *singlevariable equalizers* discussed in the first part of the chapter.

4.1 Singlevariable equalizers

4.1.1 General discussion

The problem is the following: given a sequence $y(t)$ and a *known* channel model

$$B(q^{-1}) = b_0 + b_1 q^{-2} + \ldots + b_n q^{-n} \ , \tag{4.1}$$

determine the transmitted sequence $\{d(t)\}$ when it is known that the received sequence is given by

$$y(t) = B(q^{-1})d(t) + v(t) \tag{4.2}$$

where $v(t)$ is white gaussian noise.[1] In addition, it is known that $d(t)$ can only attain a finite number of values. These assumptions will be used in the sequal.

There are basically two ways to accomplish this. One principle is to process $y(t)$ through a filter, which is a IIR filter in the general case. The filter's job is to produce an estimate of the transmitted symbol. The filtered value is then fed into a *decision device*. In the decision device, it is decided which symbol was transmitted, by the minimum of the euclidian distance to a symbol.

In some algorithms, previously decided symbols are also used in the filtering. This is called *decision feedback*.

[1] Cochannel interference can not be considered because of the assumption of white, Gaussian measurement noise. How to handle cochannel interference is described in [16].

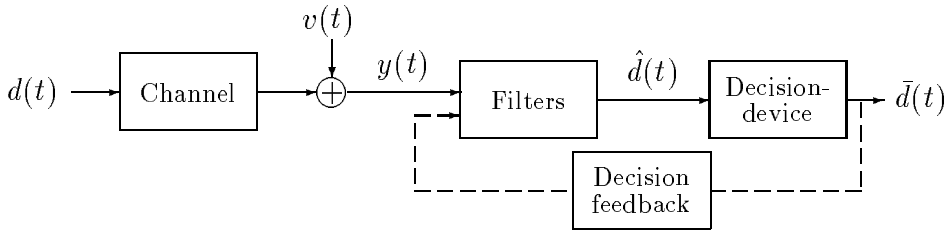

Figure 4.1: The equalization of a radio channel using a linear filtering approach.

The other principle is to estimate the transmitted symbols directly from a sequence of measurements $\{y(t)\}$. This is done by choosing the values of a sequence $\{d(t)\}$, which would lead to the values closest to the observed sequence $\{y(t)\}$. When the noise is white Gaussian, this method is equivalent to Maximum Likelihood (ML) estimation of the symbols. This method would be very complex if it was not for the *Viterbi algorithm*, which will be studied in Section 4.1.4. For a more elaborate discussion about these methods see e.g. [12].

An equalizer can be obtained in many ways. A common approach, however, is to use some sort of criterion. The two most common strategies is to optimize the mean square error (MSE) criterion or the zero forcing (ZF) criterion. The latter completely eliminates the intersymbol interference, while the MSE criterion balances removal of ISI against noise amplification.

4.1.2 Linear equalizers

The linear estimator produces an estimate $\hat{d}(t)$ of the symbol $d(t)$ from noisy measurements $\{y(t)\}$. This is done by using a stable, linear filter $\mathcal{C}(q^{-1})$, which may be rational:

$$\hat{d}(t) = \mathcal{C}(q^{-1})y(t) \ . \tag{4.3}$$

At first glance, it might seem natural to choose

$$\mathcal{C}(q^{-1}) = \frac{1}{B(q^{-1})} \ .$$

This would lead to an estimate

$$\hat{d}(t) = d(t) + \frac{1}{B(q^{-1})}v(t)$$

which is totally free of intersymbol interference. This choice is made according to the ZF criterion previously mentioned.

However, this approach has two major drawbacks:

1. There is no guarantee that $\mathcal{C}(q^{-1})$ is stable. This is often not the case when $|b_0|$ is small, compared to the other taps in the channel.

2. Even if the channel *was* minimum phase, zeros in the channel, which lie close to the unit circle, would produce large noise amplification in some parts of the spectrum. This is also a common situation in a multipath RF channel.

If the MSE criterion is used instead, the aim is to minimize the expectation of the total estimation error:

$$\mathcal{C}_{MSE} = \arg \min_{\mathcal{C}(q^{-1})} E|z(t)|^2 \tag{4.4}$$

where

$$z(t) = d(t) - \hat{d}(t) = [1 - \mathcal{C}(q^{-1})B(q^{-1})]d(t) - \mathcal{C}(q^{-1})v(t) \ .$$

It is fruitful to rewrite the problem in the frequency domain. Using Parsevals relation, and assuming $\mathcal{C}(z^{-1})$ to be stable, $E|z(t)|^2$ can be written

$$E|z(t)|^2 = \frac{\sigma_d^2}{2\pi\jmath} \oint_{|z|=1} |1 - \mathcal{C}(z)B(z)|^2 \frac{dz}{z} + \frac{\sigma_v^2}{2\pi\jmath} \oint_{|z|=1} |\mathcal{C}(z)|^2 \frac{dz}{z} \ . \tag{4.5}$$

If infinitely many measurements were available, the solution minimizing (4.5) would be given by the unrealizable *Wiener filter*:

$$\mathcal{C}(z) = \frac{B_*(z)}{|B(z)|^2 + \nu} \qquad \nu = \frac{\sigma_v^2}{\sigma_d^2} \tag{4.6}$$

$$\sigma_d^2 = E[|d(t)|^2|] \qquad \sigma_v^2 = E[|v(t)|^2|] \ .$$

Unfortunately, infinitely many data will not be available. The necessity of causality and finite delay in the transmission, requires the introduction of a *smoothing lag* m_f in the estimator:

$$\hat{d}(t) = \mathcal{C}(q^{-1})y(t + m_f) = q^{m_f}\mathcal{C}(q^{-1})y(t) \qquad m_f \geq 0 \ . \tag{4.7}$$

The smoothing lag allows signal energy, originating from one symbol, to be collected during a period of m_f samples after its first appearance at the receiver, before the estimate is calculated; hence the filter uses more information (compared to $m_f = 0$) when it estimates the symbol. Bear in mind, the first coefficient b_0 in the impulse response of the channel might not be the largest.
Next, the choice must be made if the equalizer is to have a finite (FIR) or infinte (IIR) impulse response. The recursive (IIR) equalizer generally requires fewer filter coefficients than the transversal (FIR) equalizer at a similar performance. The discussion hereafter will be devoted to the IIR equalizer.

Rewrite the filter $\mathcal{C}(q^{-1})$ as

$$\mathcal{C}(q^{-1}) = \frac{S(q^{-1})}{R(q^{-1})} \ . \tag{4.8}$$

The filter $R(q^{-1})$ is of order n, and is determined by a spectral factorization of the power spectrum $\phi_y(z)$:

$$\phi_y(z) = \sigma R(z^{-1})R(z) = B(z^{-1})B(z) + \nu \tag{4.9}$$

where ν is defined in (4.6) above. The constant σ is used for making $R(q^{-1})$ monic (unit leading coefficient). The *forward filter* $S(q^{-1})$ is calculated from the linear polynomial equation

$$q^{-m_f}B_*(q) = \sigma R_*(q)S(q^{-1}) + qL_*(q) \tag{4.10}$$

and is of order m_f. Above, $L_*(q)$ is second unknown polynomial in q to be determined. Equations (4.9) and (4.10) constitute the filter design equations. Introduce the *feedback filter* $\bar{R}(q^{-1})$:

$$\bar{R}(q^{-1}) = q(R(q^{-1}) - 1) \ .$$

With $\mathcal{C}(q^{-1})$ given by (4.8), the estimate (4.7) is given by

$$\hat{d}(t) = q^{m_f} S(q^{-1}) y(t) - \bar{R}(q^{-1}) \hat{d}(t-1) \ . \tag{4.11}$$

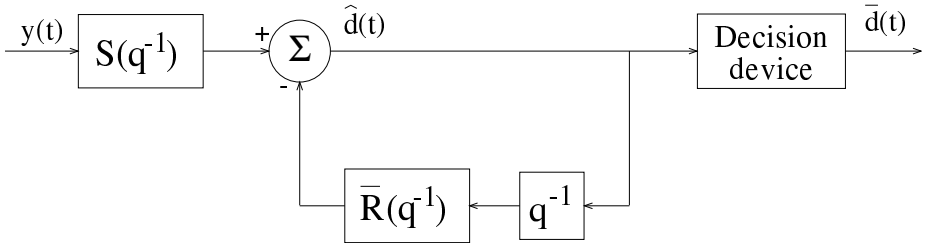

Figure 4.2: The Linear Feedback Equalizer.

This is the *Linear Feedback Equalizer* (LFE). A multivariable generalization of the LFE is discussed in e.g. [2] or [1]. The major disadvantage with it, is that it does not use the a priori information that the data are digital. This is exactly what the DFE (*Decision Feedback Equalizer*) does.

4.1.3 The decision feedback equalizer

By using *decisioned* symbols in the feedback filter, the effect of previously detected symbols on the current measurement can be eliminated. Unlike the LFE, the noise that was present in $\hat{d}(t)$ does not enter the feedback path (unless incorrect decisions are made) and hence does not affect future decisions. If this method is used in its simplest way, the expression for $\hat{d}(t)$ becomes

$$\hat{d}(t) = \frac{1}{b_0}[y(t) - \sum_{k=1}^{n} b_k \bar{d}(t-k)] \ . \tag{4.12}$$

This expression is obtained by simply inserting (4.1) into (4.2) and rearranging. If past symbols were detected correctly, this would lead to the estimate

$$\hat{d}(t) = d(t) + \frac{1}{b_0} v(t)$$

which clearly contains no intersymbol interference, much like the linear equalizer, derived from the ZF criterion. Since the feedback path is broken by the decision device, which is extremely non-linear, all signals are bounded, and no instability will occur. If correct past decisions are assumed, the feedback filter could actually be considered to be a forward filter from the transmitted symbols. See Figure 4.1.3.

If $|b_0| \neq 0$, this equalizer is stable. However, if b_0 is small, the noise will be severely amplified. To overcome this problem, the same technique as in the case of

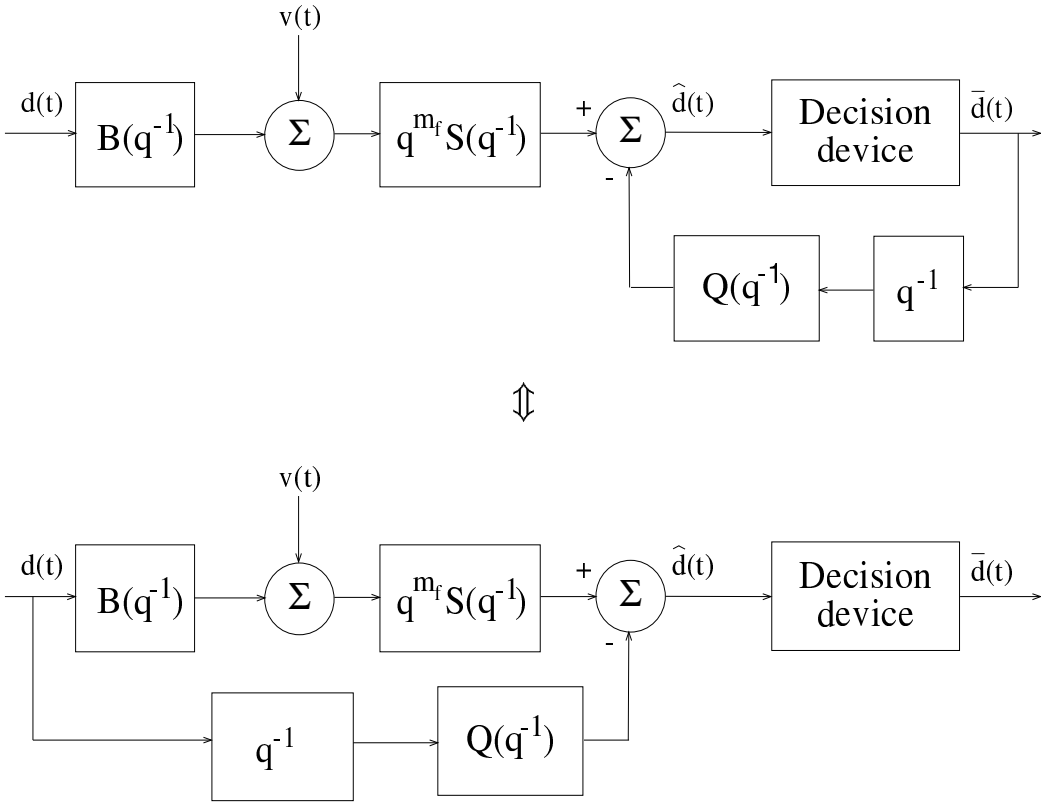

Figure 4.3: The DFE as a feedback filter and a feedforward filter.

the LFE is used: introduce a smoothing lag and construct a forward filter $S(q^{-1})$, which extracts more information from the signal $y(t)$. The expression for $\hat{d}(t)$ then becomes:

$$\hat{d}(t) = S(q^{-1})y(t) - Q(q^{-1})\bar{d}(t-1) \ . \tag{4.13}$$

Under the assumption of white measurement noise, $S(q^{-1})$ and $Q(q^{-1})$ are FIR filters. The optimal order of $S(q^{-1})$ is equal to the selected smoothing lag m_f, and the optimal order of $Q(q^{-1})$ is equal to the length of the channel impulse response minus one, i.e. $n-1$.

Inserting the expression for $y(t)$ into (4.13) gives

$$\hat{d}(t) = q^{m_f}S(q^{-1})B(q^{-1})d(t) + q^{m_f}S(q^{-1})v(t) - Q(q^{-1})\bar{d}(t-1) \ . \tag{4.14}$$

Split the filter preceding $d(t)$ into a non-causal part $G_-(q)$ of order m_f and a causal part $q^{-1}G_+(q^{-1})$:

$$q^{m_f}S(q^{-1})B(q^{-1}) = G_-(q) + q^{-1}G_+(q^{-1}) \tag{4.15}$$

where

$$G_-(q) = g_{-m_f}q^{m_f} + \ldots + g_{-1}q + g_0 \qquad G_+(q^{-1}) = g_1 + g_2q^{-1} + \ldots + g_{n-1}q^{n-1} \ .$$

If correct past decisions are assumed, the choice

$$Q(q^{-1}) \equiv G_+(q^{-1}) \tag{4.16}$$

removes all the intersymbol inteference caused by previously detected symbols. Once $S(q^{-1})$ is selected, the feedback filter is uniquely determined by (4.15) and (4.16).

As in the case of the LFE, the forward filter can be calculated by means of an MSE optimization if correct past decisions are assumed. The solution of the problem can be expressed in the following way, see [12],

1. Solve the linear system of equations

$$[\nu \mathbf{I} + \mathbf{B}_-^* \mathbf{B}_-]\theta_s = \underline{b}^* \tag{4.17}$$

where

$$\mathbf{B}_- \triangleq \begin{pmatrix} b_0 & \dots & 0 \\ \vdots & \ddots & \vdots \\ b_{m_f} & \dots & b_0 \end{pmatrix}$$

$$\underline{b}^* = (b_{m_f}, \dots, b_0)^*$$

$$\theta_s = (s_0, \dots, s_{m_f})^T \ .$$

2. Calculate the feedback filter $\theta_q = (q_1, \dots, q_{n-1})^T$ through the multiplication

$$\theta_q = B_+ \theta_s \tag{4.18}$$

where

$$\mathbf{B}_+ \triangleq \begin{pmatrix} b_{m_f+1} & \dots & b_2 & b_1 \\ 0 & & \vdots & \vdots \\ \vdots & & b_n & b_{n-1} \\ 0 & \dots & 0 & b_n \end{pmatrix} \ .$$

If $n < m_f$, the coefficients b_k, $n < k \leq m_f$ are simply set equal to zero.

The DFE calculated from (4.17) and (4.18) gives the optimal DFE only for the case of FIR channel and white or autoregressive measurement noise. In other cases, both the forward and feedback filters are in general IIR filters. This general DFE is discussed in [16]. Note that in contrast to the LFE, the calculation of the optimal DFE requires no spectral factorization, but only a solution of a linear system of equations of order $m_f + 1$.

A major drawback with the DFE is that a single erroneous decision causes the probability for further errors to increase substantially. This higher error probability can cause another error with accompaning increase in error probability. This can result in a burst of errors. Most coding strategies are rather sensitive to such bursts, and this forces the radio system to use *interleaving*. Interleaving is a coding technique, which separates adjacent symbols, so that they will not fall into the same error burst. However, interleaving causes a delay in the transmission, and a delay is always unwelcome. In [17], so-called *robust equalizers* are discussed. These algorithms can, among other things, control the error bursts, and can basically trade shorter, but more frequently occuring error bursts for the longer, but seldomly occuring ones.

4.1.4 The Viterbi algorithm

As mentioned earlier, the Viterbi algorithm selects the symbol sequence, which provides a channel output signal sequence closest to the real one. This algorithm was not developed to equalize multipath fading channels. Originally, it was devised to decode convolution codes, but found another suitable application. This section will only give a short introduction to the idea of the Viterbi algorithm. For a more thorough treatment, see [12], [13].

The criterion minimized by the Viterbi algorithm is

$$\{\hat{d}_t\}_{t=1}^{N} = \arg \min_{\{d_t\}_1^N} \sum_{t=1}^{N} |y_t - \hat{y}(\hat{d}_t, \hat{d}_{t-1}, \ldots, \hat{d}_{t-n})|^2 \tag{4.19}$$

where $\{y_t\}_1^N$ is the received sequence and $\{\hat{y}_t\}_1^N$ is the output of the noise-free channel model

$$\hat{y}(\hat{d}_t, \hat{d}_{t-1}, \ldots, \hat{d}_{t-n}) = \sum_{k=0}^{n} b_k d_{t-k} \ .$$

The Viterbi algorithm uses the limited length of the channel impulse response; hence, the algorithm is difficult to use on IIR channels. In an iterative manner, it calculates *branch metrics*, which should be as small as possible for an alternative to have large probability. Define

$$\gamma_t(d_1, d_2, \ldots, d_{n+1}) \triangleq \sum_{k=1}^{t} |y_k - \hat{y}(d_k, d_{k-1}, \ldots, d_{k-n})|^2 \quad t \leq n+1 \tag{4.20}$$

$$d_t \equiv 0 \qquad \forall t \leq 0$$

$$\gamma_t(d_{t-n}, d_{t-n+1}, \ldots, d_t) \triangleq |y_t - \hat{y}(d_t, d_{t-1}, \ldots, d_{t-n})|^2 \quad t > n+1 \ . \tag{4.21}$$

Equation (4.19) can then be written

$$\{\hat{d}_t\}_{t=1}^{N} = \arg \min_{\{d_t\}_1^N} \sum_{t=n+1}^{N} \gamma_t(d_{t-n}, d_{t-n+1}, \ldots, d_t) \ . \tag{4.22}$$

As the time N increases, the required number of metrics would grow without limit, since the number of alternatives grows exponentially. If the alphabet consists of M symbols, each symbol arriving at the receiver would require M times as many metric calculations as the preceding symbol.

The Viterbi algorithm, which constitutes forward dynamic programming, finds a way to reject some of the possible combinations of symbols. Consider a FIR channel with an impulse response of length three. In an iterative way, the metrics of the M^3 possible combinations of the three first symbols are calculated. Since γ_4 does not depend on the first symbol d_1, it is possible to rule out some of the possibilities *before even calculating* γ_4. This is done by grouping the sequences so that they only differ in the first position, i.e. in d_1. After that, the metrics of the pairs of sequences are compared, and the alternative *within each pair* which has the largest metric is discarded. In this way, the number of calculations in each step becomes bounded and does not increase with the sequence length N. See [12]

for a more elaborate discussion.

Since the Viterbi algorithm basically is a sequence estimator, it introduces a time delay. In a telephone system, this is a drawback. It is however possible to use a modified algorithm which makes it possible to make decisions on a symbol-by-symbol basis, which admits real time implementation.

The main drawback of the Viterbi algorithm is still its complexity. The complexity grows exponentially with the channel length. Likewise, it grows exponentially with the size of the symbol alphabet.

4.1.5 Comparison

The performance of the three studied methods is compared in Figure 4.4 for a multipath propagation channel with severe intersymbol interference. It should be stressed however, that the performance can vary *considerably* when the conditions change. When fading characteristics (i.e. the inability to guarantee a fixed SNR) are introduced, the difference between the DFE and the Viterbi algorithm at higher SNRs decreases instead of increases. But it shows the two major points, when comparing equalizer structures: the LFE is inferior to the other two and the Viterbi algorithm is a little bit better than the DFE.

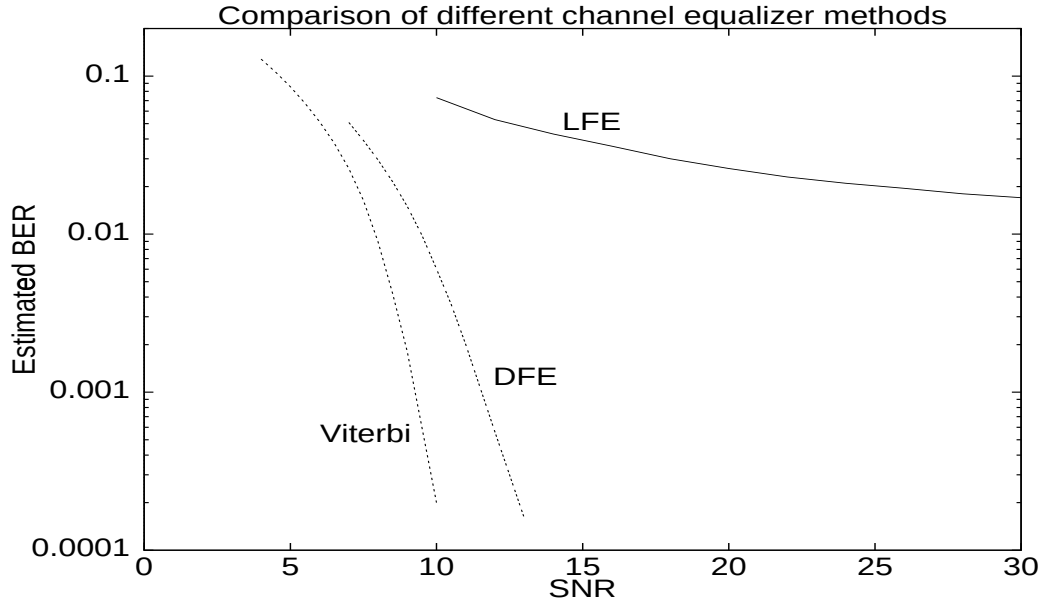

Figure 4.4: Comparison of the performance (BER) of the three discussed equalizing methods for a typical multipath propagation channel (from [3]).

The LFE is clearly inferior to the other two. The Viterbi algorithm is the most powerful method, but for BER typical for mobile radio communications, the difference is negligable. In studies of propagation models relevant to both the ADC and GSM systems, the difference in performance between the DFE and the Viterbi algorithm is much smaller than the difference displayed in Figure 4.4.

4.2 Multivariable equalizing

Since the LFE clearly performes quite badly, our candidates for a multivariable equalizer are the DFE and the Viterbi algorithm.

4.2.1 The multivariable DFE

The multivariable DFE is not very different from the singlevariable version. However, the coefficients of the channel are not scalars any more. In the general case, if the number of antennas are n_y and the number of messages are n_d, the channel coefficients are of dimension $n_y|n_d$, the coefficients of the forward filter $\boldsymbol{S}(q^{-1})$ are of dimension $n_d|n_y$ and the coefficients of the feedback filter $\boldsymbol{Q}(q^{-1})$ are of dimension $n_d|n_d$:

$$\begin{pmatrix} y_1(t) \\ \vdots \\ y_{n_y}(t) \end{pmatrix} = (\mathbf{B}_0 + \mathbf{B}_1 q^{-1} + \ldots + \mathbf{B}_n q^{-n}) \begin{pmatrix} d_1(t) \\ \vdots \\ d_{n_d}(t) \end{pmatrix} + \begin{pmatrix} v_1(t) \\ \vdots \\ v_{n_y}(t) \end{pmatrix} \tag{4.23}$$

$$\begin{aligned} \begin{pmatrix} \hat{d}_1(t) \\ \vdots \\ \hat{d}_{n_d}(t) \end{pmatrix} &= q^{m_f}(\mathbf{S}_0 + \mathbf{S}_1 q^{-1} + \ldots + \mathbf{S}_{m_f} q^{-m_f}) \begin{pmatrix} y_1(t) \\ \vdots \\ y_{n_y}(t) \end{pmatrix} \\ &- (\mathbf{Q}_0 + \mathbf{Q}_1 q^{-1} + \ldots + \mathbf{Q}_{n-1} q^{-(n-1)}) \begin{pmatrix} \bar{d}_1(t-1) \\ \vdots \\ \bar{d}_{n_d}(t-1) \end{pmatrix} \end{aligned} \tag{4.24}$$

where the matrix coefficients of the polynomials have dimensions

$$\mathbf{B}_k = \underbrace{\begin{pmatrix} \bullet \end{pmatrix}}_{n_d} \Big\} n_y \qquad \mathbf{S}_k = \underbrace{\begin{pmatrix} \bullet \end{pmatrix}}_{n_y} \Big\} n_d \qquad \mathbf{Q}_k = \underbrace{\begin{pmatrix} \bullet \end{pmatrix}}_{n_d} \Big\} n_d \ .$$

When the DFE is calculated, it is possible to follow the same procedure as when calculating the singlevariable DFE, replacing the scalars with matrices. But to show an alternative derivation, the following algorithm can be used to calculate the forward filter.

Theorem 4.1
Assume the channel is given by (4.23). Assuming correct past decisions, the FIR DFE given by (4.24), minimizing the filtering error

$$\underline{z}(t) = \underline{d}(t) - \underline{\hat{d}}(t)$$

in the MSE sense, has the matrix coefficients given by the following algorithm.

1. Solve the system of linear equations

$$\left(\begin{array}{cccc|cccc} \mathbf{B}_0^T & \mathbf{0} & \dots & \mathbf{0} & \mathbf{I}_{n_d} & \mathbf{0} & \dots & \mathbf{0} \\ \mathbf{B}_1^T & \mathbf{B}_0^T & \dots & \mathbf{0} & \mathbf{0} & \mathbf{I}_{n_d} & \ddots & \mathbf{0} \\ \mathbf{B}_2^T & \mathbf{B}_1^T & \ddots & \mathbf{0} & \mathbf{0} & \ddots & \ddots & \mathbf{0} \\ \vdots & \vdots & \ddots & \vdots & \vdots & \vdots & \ddots & \vdots \\ \mathbf{B}_{m_f}^T & \mathbf{B}_{m_f-1}^T & \dots & \mathbf{B}_0^T & \mathbf{0} & \mathbf{0} & \dots & \mathbf{I}_{n_d} \\ \hline -\Psi^T & \mathbf{0} & \dots & \mathbf{0} & \bar{\mathbf{B}}_0 & \bar{\mathbf{B}}_1 & \dots & \bar{\mathbf{B}}_{m_f} \\ \mathbf{0} & -\Psi^T & \dots & \mathbf{0} & \mathbf{0} & \bar{\mathbf{B}}_0 & \dots & \bar{\mathbf{B}}_{m_f-1} \\ \vdots & \vdots & \ddots & \vdots & \vdots & \vdots & \ddots & \vdots \\ \mathbf{0} & \mathbf{0} & \dots & -\Psi^T & \mathbf{0} & \mathbf{0} & \dots & \bar{\mathbf{B}}_0 \end{array}\right) \left(\begin{array}{c} \mathbf{S}_0^T \\ \mathbf{S}_1^T \\ \mathbf{S}_2^T \\ \vdots \\ \mathbf{S}_{m_f}^T \\ \hline \bar{\mathbf{L}}_{1m_f} \\ \bar{\mathbf{L}}_{1(m_f-1)} \\ \vdots \\ \bar{\mathbf{L}}_{10} \end{array}\right) = \left(\begin{array}{c} \mathbf{0} \\ \mathbf{0} \\ \vdots \\ \mathbf{0} \\ \mathbf{I}_{n_d} \\ \hline \mathbf{0} \\ \mathbf{0} \\ \vdots \\ \mathbf{0} \end{array}\right) \tag{4.25}$$

where

$$\Psi = E[\underline{v}(t)\underline{v}(t)^*] \ .$$

and the zeroes on the right hand side are matrices of dimension $n_d|n_d$, for the matrix coefficients $\mathbf{S}_i,\ i = 0,1,\dots,m_f$ and $\mathbf{L}_{1i},\ i = 0,1,\dots,m_f$.

2. Perform the following matrix multiplication:

$$\begin{pmatrix} \mathbf{Q}_0 & \mathbf{Q}_1 & \dots & \mathbf{Q}_{n-1} \end{pmatrix} =$$

$$= \begin{pmatrix} \mathbf{S}_{m_f} & \mathbf{S}_{m_f-1} & \dots & \mathbf{S}_0 \end{pmatrix} \times \begin{pmatrix} \mathbf{B}_1 & \mathbf{B}_2 & \dots & \dots & \dots & \mathbf{B}_n \\ \mathbf{B}_2 & \mathbf{B}_3 & \dots & \dots & \mathbf{B}_n & \mathbf{0} \\ \vdots & \ddots & \dots & \dots & \dots & \vdots \\ \mathbf{B}_{m_f+1} & \dots & \mathbf{B}_n & \mathbf{0} & \dots & \mathbf{0} \end{pmatrix} . \tag{4.26}$$

■

Proof: See Appendix C.

Remark 1. As in the case of the singlevariable equalizer, if $n < m_f$ the matrix coefficients of $\boldsymbol{B}(q^{-1})$ of degree higher than m_f in (4.25) and (4.26) are simply set to zero.

Remark 2. Equation (4.25) can be divided into block matrix form, and hence written

$$\begin{pmatrix} \mathbf{A}^T & \mathbf{I} \\ -\mathbf{D} & \bar{\mathbf{A}} \end{pmatrix} \begin{pmatrix} \mathbf{E} \\ \mathbf{F} \end{pmatrix} = \begin{pmatrix} \mathbf{J} \\ \mathbf{0} \end{pmatrix} .$$

where the corresponding blocks have been indicated in (4.25). Thus

$$\begin{aligned} \mathbf{A}^T\mathbf{E} + \mathbf{F} &= \mathbf{J} \\ -\mathbf{D}\mathbf{E} + \bar{\mathbf{A}}\mathbf{F} &= \mathbf{0}. \end{aligned}$$

Multiply the first equation by $\bar{\mathbf{A}}$ from the left. Insert the product $\bar{\mathbf{A}}\mathbf{F}$ from the second equation into the first. This gives

$$(\bar{\mathbf{A}}\mathbf{A}^T + \mathbf{D})\mathbf{E} = \bar{\mathbf{A}}\mathbf{J} \ . \tag{4.27}$$

Perform the multiplication on the right hand side. Equation (4.27) is then reduced to

$$(\mathbf{D} + \bar{\mathbf{A}}\mathbf{A}^T)\mathbf{E} = \begin{pmatrix} \bar{\mathbf{B}}_{m_f} \\ \vdots \\ \bar{\mathbf{B}}_0 \end{pmatrix} . \tag{4.28}$$

Equation (4.28) is the multivariable equation corresponding to the singlevariable (4.17). Equation (4.28) has the obvious advantage of having dimension $n_d(m_f + 1)$ instead of $(n_d + n_y)(m_f + 1)$ for (4.25). A matrix inversion is an operation with a numerical complexity which is proportional to N^3, where N is the size of the matrix. Reducing the size of the matrix by a factor two hence reduces the computation time by a factor of eight. Notice also that the complexity is minimized by the fact that the linear system of equations in (4.25) (and (4.28)) is solved for multiple right hand sides, only requiring one LU-decomposition. An alternative would have been to stack the elements of the matrix coefficients on top of one another. However, this would have resulted in n_d times longer vector of unknowns, and a correspondingly larger matrix to invert.

The algorithm above can be used for any number of antennas (n_y) and messages (n_d). For instance, when $n_y = 2$ and $n_d = 1$, it provides the optimal combiner for two antennas and one message; hence *this DFE can be interpreted as the maximum ratio combiner for the case of arbitrarily severe intersymbol interference.*

It is possible to generalize the above result to IIR channels, colored symbols and also to arbitrarily colored noise.

Equation (4.25) has a unique solution for any combination of n_y and n_d if Ψ has full rank. If some measurements are considered noise-free, solvability may, however, not be possible to guarantee.

4.2.2 Why not a multivariable Viterbi detector?

Since the Viterbi detector theoretically is the most powerful detector, it would of course be interesting to see how it performs in the case of a multivariable channel. However, the complexity of the algorithm puts obstacles in the way. Introducing a multivariable channel means, that the number of metric branches that must be calculated increases. In fact, the complexity of a Viterbi detector for a message vector $\underline{d}(t) = (d_1\ d_2\ \ldots\ d_{n_d})^T$ with an alphabet of M symbols is equivalent to the complexity of a singlevariable Viterbi detector for an alphabet of M^{n_d}, and the number of metrics to be calculated is increased accordingly. This would lead to a very high complexity indeed. Hence our candidate for multivariable channel equalization is the DFE.

Remark. In [8], a *suboptimal* Viterbi detector is derived for the case of one receiver antenna and two transmitters. This approach reduces the computational complexity at the expense of an increased BER.

Chapter 5

A simulation study

All the simulations that will be mentioned in this chapter were performed using a special library for matrices and matrix functions, developed at the Systems and Control Group, Uppsala University. This library was written in C++ during the spring of 1993.

5.1 The deterministic model

5.1.1 Statement of the problem

The model used in this chapter is the deterministic model of Section 3.2, and hence only the uplink is studied. The system under consideration is thus

$$\underline{y}(t) = \boldsymbol{B}(q^{-1})\underline{d}(t) + \underline{v}(t) \ .$$

The following assumptions that were made:

1. There are two transmitters (mobiles) and at the base station, there exist two receiver antennas. This means that the dimension of the channel coefficients $\mathbf{B}_k$ is $2|2$.

2. The channel has only one tap; hence there is no intersymbol interference.

3. The channel coefficient has the following structure:

$$\mathbf{B}_0 = \begin{pmatrix} b_1 & b_2 \\ b_1 & b_2 e^{-\jmath\Delta\varphi} \end{pmatrix} \tag{5.1}$$

   where b_1 and b_2 are positive real numbers. Thus, the received signals at the base station are given by:

$$\begin{aligned} y_1(t) &= b_1 d_1(t) + b_2 d_2(t) + v_1(t) \\ y_2(t) &= b_1 d_1(t) + b_2 e^{-\jmath\Delta\varphi} d_2(t) + v_2(t) \ . \end{aligned}$$

4. The complex noise vector $\underline{v}(t) \in \mathcal{CN}(\mathbf{0}, \mathbf{I})$ is white and uncorrelated with the transmitted symbols.

5. The mutually uncorrelated symbols $\{d(t)\}$ belong to the set {-1,1}, and the probability for each of these values is equal.

In Section 3.2, it is mentioned that the resulting BER depends only on the phase difference $\Delta\varphi_1 = \varphi_2 - \varphi_1$. (See also Appendix B.) This is also a motivation for b_1 and b_2 being real numbers, which also is intuitively appealing.

The restriction to a single-tap channel might seem oversimplified, but actually it is the worst case. In case of a channel with multiple taps, it does not matter if some of the taps are badly conditioned, just as long as all of them are not.

5.1.2 The simulation

The simulations were performed with

- $\Delta\varphi \in [0, \pi]$.
- $b_1 \in [1, 10]$ (This corresponds to SNR=E$[\frac{|b_1 d_i(t)|^2}{|v_i(t)|^2}] \in$ [0dB,20dB].).
- $b_2 \in [1, 10]$ (This corresponds to SNR=E$[\frac{|b_2 d_i(t)|^2}{|v_i(t)|^2}] \in$ [0dB,20dB].).

The first conclusion that could be drawn was that the resulting BER's were symmetrical: it did not matter whether transmitter number one or transmitter number two was the strongest. This is quite natural.

Next, when one transmitter was made stronger, estimation of that signal produced fewer errors. The weaker transmitter quite naturally showed the opposite behavior. In fact, the *total* BER did not change if the power of the stronger transmitter was changed as long as it *remained* the stronger, i.e. the total BER was only effected by the SNR of the *weakest* signal. Hence, the ratio between the two SNR's was not an interesting parameter (for the total BER), and the results presented in this section are for transmitters of equal strength. This is also the relation which should be used in practice, since it is desirable to distribute the total BER evenly among the involved mobiles, in order to achieve reasonable speech-quality for both. This is even more so, since digital telephone systems have a threshold BER, under which the speech quality decreases abruptly.

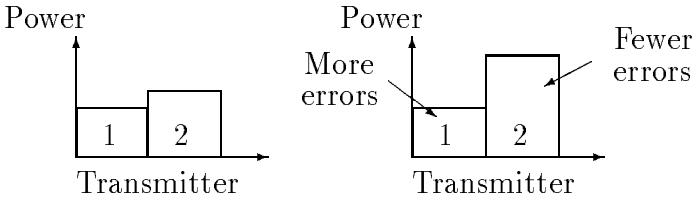

Figure 5.1: The result of increasing the transmitter power of one transmitter while keeping the other constant.

The single remaining interesting parameter is thus the SNR of the weakest signal. The BER as a function of the phase difference $\Delta\varphi$ with SNR as the parameter is shown in Figure 5.2.

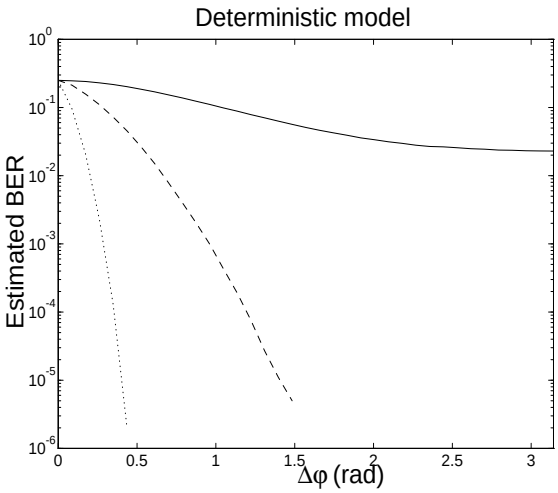

Figure 5.2: The BER as a function of $\Delta\varphi$ for SNR=0dB (solid), SNR=10dB (dashed) and SNR=20dB (dotted).

As stated in Section 3.2, the phases φ_1 and φ_2 are related to the incoming angles α_i by

$$\varphi_i = 2\pi \frac{s}{\lambda} \cos \alpha_i \qquad i = 1, 2 \ .$$

where s is the distance between the antennas.

5.1.3 Verification

Having achieved these results from simulations, it would be nice to be able to verify the results in some way. For the deterministic model, one could analytically calculate the probability of error. This is accomplished through setting up the joint probability density function for the vector $\underline{d} = (d_1\ d_2)^T$, and checking what conditions must be fulfilled in order to obtain an erroneous decision. The calculation was carried out for $b_1 = b_2 = 1$, and the result is given in Result 5.1.

Result 5.1. With $b_1 = b_2 = 1$, together with the other conditions in this section, the probability of error and hence the BER is given by

$$P_{wrong}(\Delta\varphi) = \frac{1}{2\sqrt{\pi}} \int_{\delta_1'}^{\infty} e^{-t^2}\, dt + \frac{1}{2\sqrt{\pi}} \int_{\delta_2'}^{\infty} e^{-t^2}\, dt \tag{5.2}$$

where

$$\delta_1' = \frac{5 - \cos\Delta\varphi}{\sqrt{10 - 8\cos\Delta\varphi}} \qquad \delta_2' = \frac{3 - 3\cos\Delta\varphi}{\sqrt{10 - 8\cos\Delta\varphi}}$$

■

Proof: See Appendix B.

The result is shown in Figure 5.3 together with the corresponding simulation.

As can be seen, there is a perfect agreement between the simulated and theoretically obtained values. This agreement can not be easily accomplished in a channel having an impulse response greater than one sample, since error bursts make the problem extremely difficult to analyze.

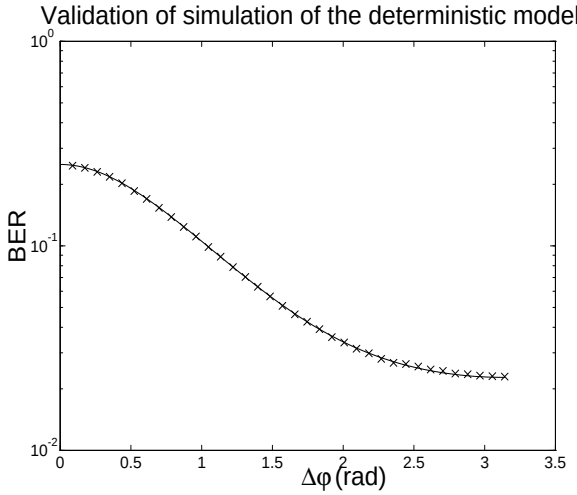

Figure 5.3: Theoretically calculated (solid) and simulated (x) BER for SNR=0dB.

5.2 The stochastic model

5.2.1 Prerequisites

In this section, we make the following assumptions:

- Assumptions 1, 4 and 5 from subsection 5.1.1 hold.
- The channel coefficients have the properties given in Section 3.3.
- The channel coefficients are assumed to be *known and time invariant.*
- Channels are accurately described by one or two taps.
- When the length of the channel impulse response is two, the two taps are assumed mutually uncorrelated.
- In the downlink case, there are two antennas at each mobile.

5.2.2 The simulations

The elements of a matrix channel coefficient

$$\mathbf{B}(x) = \begin{pmatrix} b_{01}^1(x) & b_{01}^2(x) \\ b_{02}^1(x) & b_{02}^2(x) \end{pmatrix} .$$

are all taken from the same Rayleigh sequence. The Rayleigh sequence is calculated by a MATLAB-program, written by Lars Lindbom, see also [12]. The two pairs of elements in the matrix which are uncorrelated (b_{01}^i and b_{02}^i in the downlink, and b_{0i}^1 and b_{0i}^2 in the uplink, $i = 1, 2$), are taken from two points of the sequence, sufficiently far apart. The two elements, which *are* correlated (b_{0i}^1 and b_{0i}^2 in the downlink, and b_{01}^i and b_{02}^i in the uplink, $i = 1, 2$), are taken at two points closely spaced. When two taps are required, they are taken from different Rayleigh sequences. The simulations were carried out under the following conditions:

- The envelope correlation varied in the interval $\rho_d \in [0.1, 1]$, $\rho_u \in [0.1, 1]$.
- SNR=5, 10, 15 and 20dB, where SNR is defined as

$$\text{SNR} = \frac{E[|b_{0k}^m(x)|^2]}{E[|v_i(t)|^2]} \qquad k, m, i = 1, 2 \tag{5.3}$$

  in the single-tap case, and

$$\text{SNR} = \frac{E[|b_{0k}^m(x)|^2] + E[|b_{1k}^m(x)|^2]}{E[|v_i(t)|^2]} \qquad k, m, i = 1, 2 \tag{5.4}$$

  in the two-tap case. In principle, eight different combinations of k, m and i *could* exist. However, since there is no reason why the power of the noise ($E[|v_i(t)|^2]$) at the two antennas should be anything but equal, only four interesting combinations remain, which depend on the channel. In this thesis, all these "different" SNR's are chosen equal.
- For each envelope correlation, 1000 channels were simulated, each with 400 symbol pairs.
- The DFE (4.23)–(4.26) was used with smoothing lag equal to the length of the channel impulse response, i.e. $m_f = n$.
- In the downlink simulations, each base station antenna transmitted a *separate* message.
- In the two-tap case, the average power (the variance) of the two taps were equal.

Since the average signal strengths of the two messages are set to be equal, the estimated BERs for the two transmitters show no significant difference. Therefore, in the graphs, only the mean of the two BER's is shown. This is the case for all simulations carried out in this section.

The uplink

The results are shown in Figure 5.4 for the single-tap case, and in Figure 5.5 for the two-tap case. In Figure 5.8, the BER is shown as a function of SNR$\in$[5dB,20dB] (defined in (5.3) and (5.4)), with the envelope correlation ρ_u as parameter.

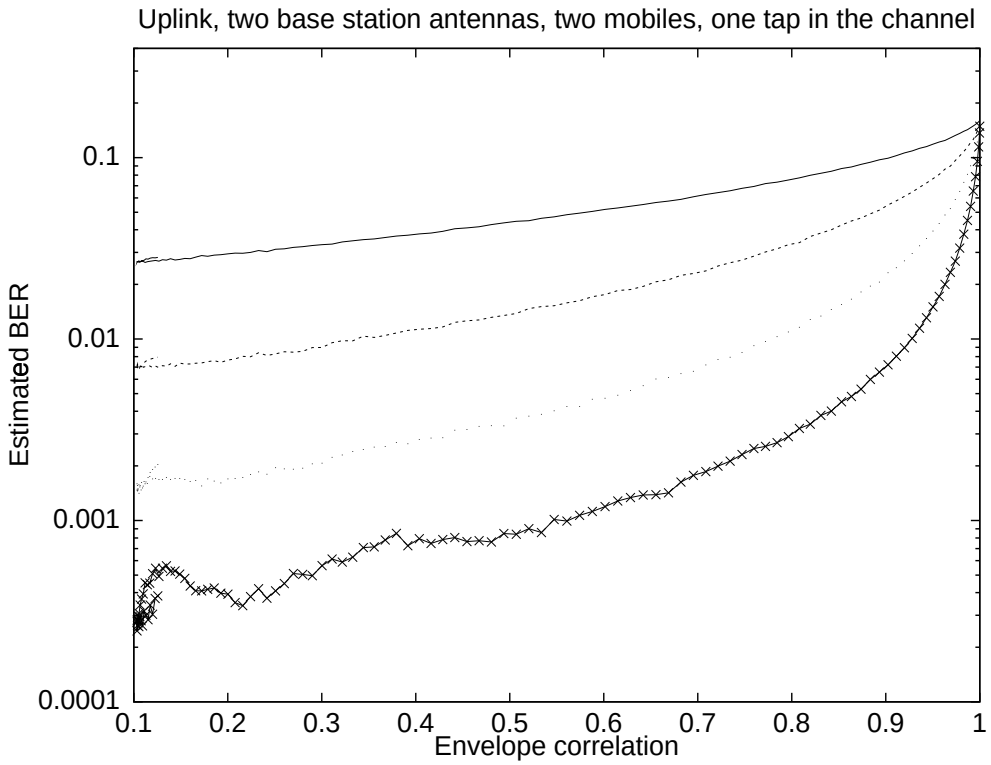

Figure 5.4: The BER as a function of envelope correlation for SNR=5dB (solid), SNR=10dB (dashed), SNR=15dB (dotted) and SNR=20dB (x-solid) for a channel with an impulse response of length one.

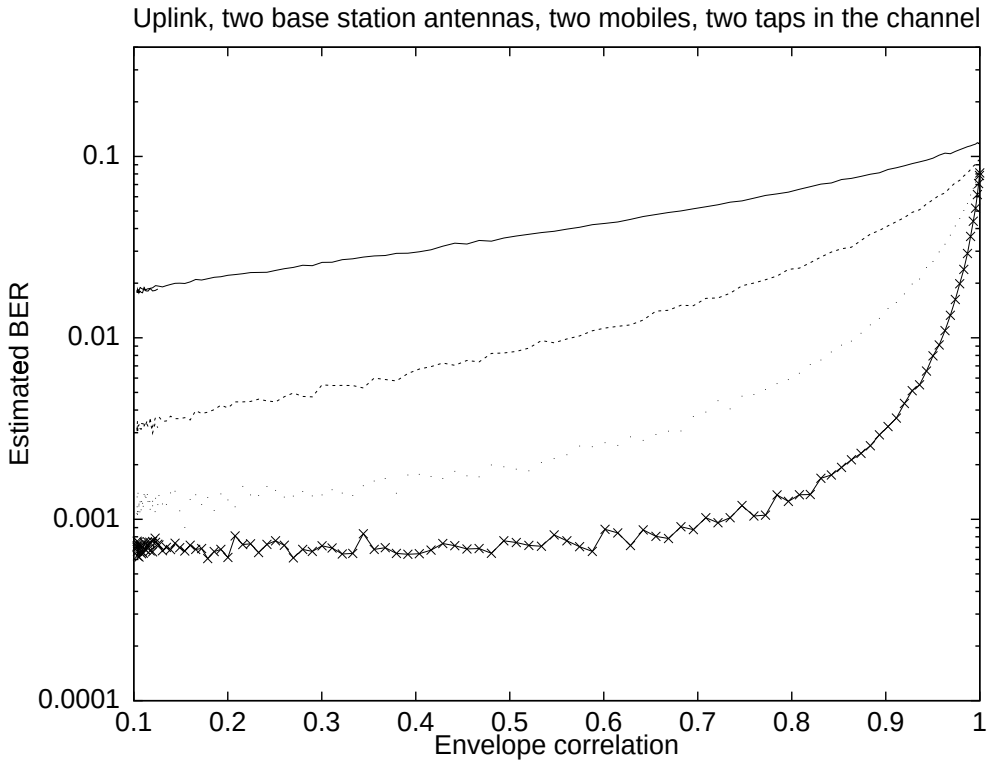

Figure 5.5: The BER as a function of envelope correlation for SNR=5dB (solid), SNR=10dB (dashed), SNR=15dB (dotted) and SNR=20dB (x-solid) for a channel with an impulse response of length two.

The downlink

The results are shown in Figure 5.6 for the single-tap case, and in Figure 5.7 for the two-tap case. In Figure 5.8, the BER is shown as a function of SNR$\in$[5dB,20dB] (defined in (5.3) and (5.4)), with ρ_d as parameter.

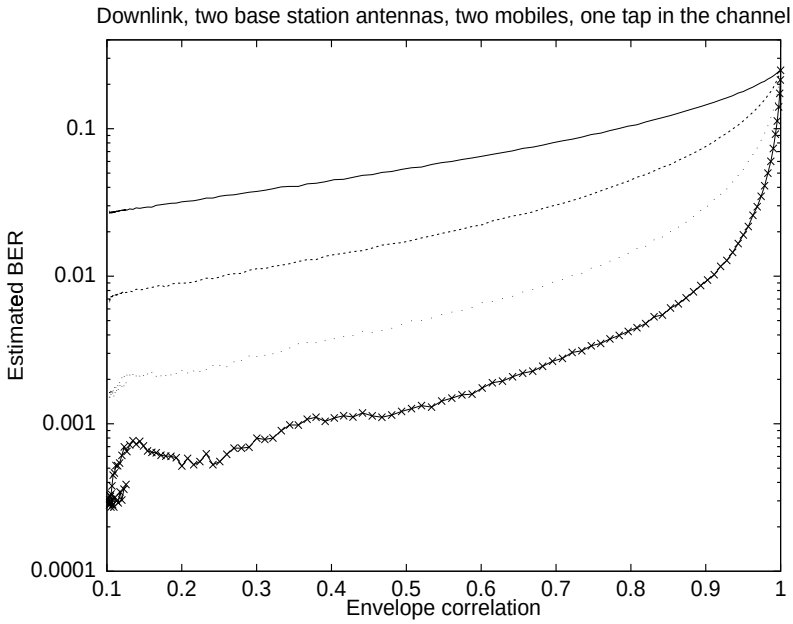

Figure 5.6: The BER as a function of envelope correlation for SNR=5dB (solid), SNR=10dB (dashed), SNR=15dB (dotted) and SNR=20dB (x-solid) for a channel with an impulse response of length one.

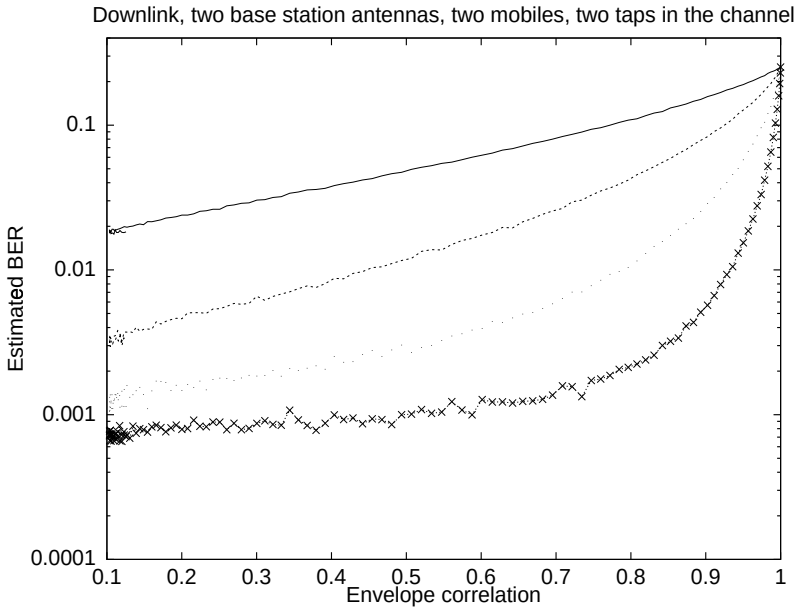

Figure 5.7: The BER as a function of envelope correlation for SNR=5dB (solid), SNR=10dB (dashed), SNR=15dB (dotted) and SNR=20dB (x-solid) for a channel with an impulse response of length two.

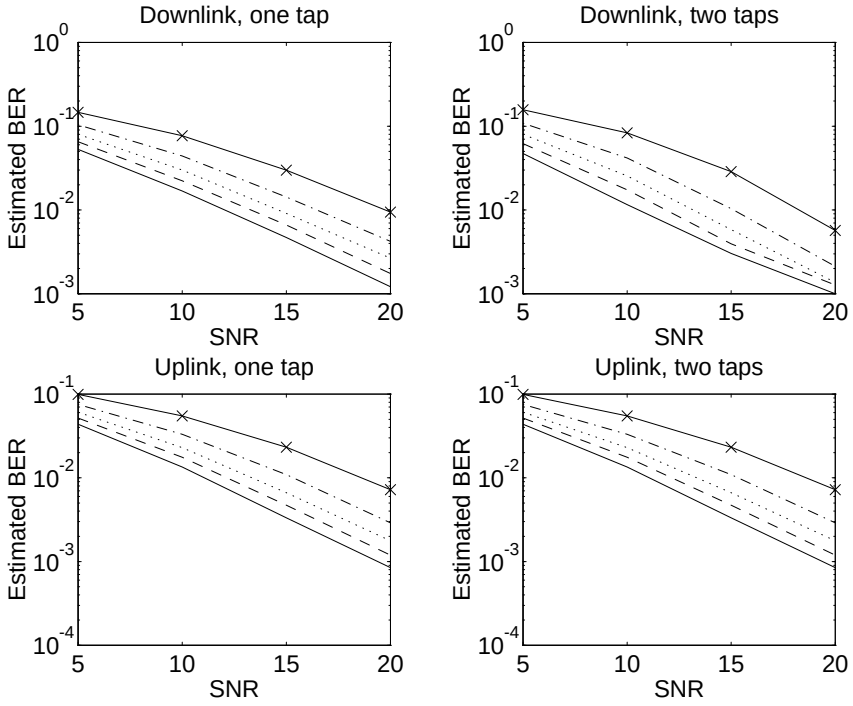

Figure 5.8: The BER as a function of SNR for an envelope correlation of 0.5 (solid), 0.6 (dashed), 0.7 (dotted), 0.8 (dash-dotted) and 0.9 (x-solid).

All graphs in Figures 5.4 to 5.7 share some properties. For envelope correlation $\rho = 1$, i.e. identical channels, the SNR does not matter. The curves all start at a BER of 25% for the downlink and ≈12% for the uplink. The major reason for erroneous decisions is then the inability of the algorithms to separate the two messages. This effect decreases very rapidly when the correlation decreases. The noise becomes the major reason for errors. This can clearly be seen as the BER curves fall off much more rapidly for higher SNR. The difference between the different BER-values is also larger for the case of a two-tap channel than in the case of a single-tap channel. The reason is that the longer the impulse response, the less likely it is that all tap matrices are badly conditioned simultaneously. Thus, multipath propagation actually *helps* this system to utilize spatial diversity.

The envelope correlation between the two antennas is cumbersome to calculate. Among other things, it depends upon the topographical environment in which the base station antenna stands, the distance between the antennas and the incoming angle of the two beams. For derivation and discussion of the correlation, see [9].

5.3 Comparison with singlevariable equalizers and conventional diversity methods

It is of course of interest to compare these results with what could be expected for today's systems. That is the subject of this section. The comparisons are made for the following two cases:

1. A system with a single mobile, having one antenna and a base station with *one antenna*.

   - Two taps in the channel, each subject to independent Rayleigh fading.
   - SNR=10dB, where the signal-to-noise ratio is defined as

$$\text{SNR} = \frac{E[|b_0|^2 + |b_1|^2]}{E[|v(t)|^2]} \ .$$

2. A system with a single mobile, having one antenna and a base station with *two antennas*, which utilize selection diversity. A comparison is also made with an optimal DFE for this case, i.e. $n_y = 2$ and $n_d = 1$ in Theorem 4.1. Simulations were made under the following assumptions:

   - Two taps in the channel.
   - The channel coefficients have the following properties:

$$b_k = \begin{pmatrix} b_k^1 \\ b_k^2 \end{pmatrix} \qquad k = 0, 1$$

$$\frac{E[|b_0^i|^2 + |b_1^i|^2]}{E[|v_i|^2]} = \text{SNR} = 10\text{dB} \qquad i = 1, 2$$

$$\frac{E[|b_k^1||b_k^2|] - E[|b_k^1|]E[|b_k^2|]}{E[|b_k^1|^2] - (E[|b_k^1|])^2} = \rho \qquad k = 0, 1 \ .$$

   In this case, the resulting BER clearly depends on the correlation between the antennas.

The results are displayed in Figure 5.9, together with results from Figures 5.5 and 5.7. Note that in the three cases used for comparison, only *one* message has to be detected, while in the case of the multivariable equalizer, *two* messages (i.e. twice the number of symbols) have been detected.

Remark In [5], an optimum decision feedback equalizer was derived by Balaban and Salz for the general diversity case with several branches. The approach taken there was also to minimize the MSE. However, the channel was not considered completely discrete in time. Rather, the prefilter of the DFE derived in [5], is continuous in time, and only the feedback path is discrete in time. This inhibits a complete and fair comparison, but since the criterion that was minimized is the same, the method should be similar to the optimum diversity DFE derived here (at least for some choices of the smoothing lag m_f). Note that [5] assumed independently fading channels. This is *not* the case for the DFE derived in this thesis. In [6], a numerical study was carried out for the optimum diversity scheme derived in [5]. That example was more realistic than the ones presented in this thesis. It included continuous-time models of the channel and the prefilter, and the operating conditions were taken from the proposed American mobile telephone system ADC previously mentioned. The resulting BER from that study were generally higher than those obtained here. This might be explained by the modulation used there (4-QAM), which has a larger alphabet; $\{1 + \jmath, 1 - \jmath, -1 + \jmath, -1 - \jmath\}$.

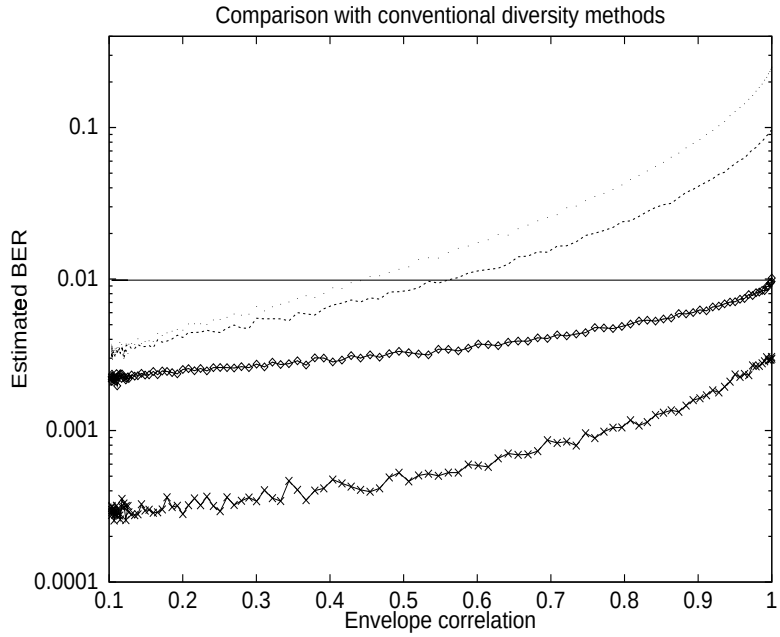

Figure 5.9: The BER for the six different situations listed above: single base station antenna (horizontal and solid), selection diversity ($\diamondsuit$-solid), multivariable, single message (x-solid) and multivariable, two messages, uplink (dashed) and downlink (dotted).

5.4 Concluding remarks

- The simulations performed with a deterministic model give extremely low BER, but is based on non-realistic assumptions, since it does not account for the fading dips in the channel.
- The BER's obtained from the stochastic model are also very low already for moderately correlated channels. The only assumptions that are made here are that the channel is known and time invariant.

The BER for an envelope correlation of 0.7 is shown in Table 5.1 for the four cases simulated in the stochastic case. The figure 0.7 is chosen quite arbitrarily.

Table 5.1: The BER at envelope correlation 0.7 in the stochastic model (two base station antennas, two mobiles, multivariable DFE).

Link	Number of taps	BER(%) SNR=5dB	BER(%) SNR=10dB	BER(%) SNR=15dB	BER(%) SNR=20dB
Uplink	1	6.1	2.3	0.66	0.18
Uplink	2	5.2	1.5	0.37	0.18
Downlink	1	8.0	3.0	0.91	0.27
Downlink	2	8.0	2.6	0.58	0.14

Chapter 6

Conclusions

6.1 Discussion of the results

The problem of being able to reuse the same frequency in the same mobile telephone cell has been addressed in this thesis. The considered system has been a digital one and a view of a discrete channel model has been adopted. It has been assumed throughout the thesis, that the base station has *two* antennas. The basic property that has been utilized, is the fact that the two transmitters have *different* channels to the receiver antennas. This has been exploited in two models, one deterministic and one stochastic.

In the *deterministic* model, the base station antennas are used as a directional antenna. The channels from one mobile to each antenna are considered to be identical, except for a phase difference, resulting from the carrier wave phase. This property has been used and the results are very good. The BER falls off very rapidly when the phase difference increases. The channel has here been considered to have a constant magnitude. This means that no local fading dips have been encountered, which explains the extremely good results.

For the deterministic model, an explicit formula for the probability of error has been derived. The results from this formula agree perfectly with the results from the simulations. The deterministic model can however only be used in the uplink. It is useless in the downlink, since no deterministic phase difference can be utilized in the Rayleigh fading environment around the mobile. The assumption of no fading dips is of course also unrealistic in most cases for the uplink. A stochastic model has thus also been studied.

The *stochastic* model assumes the mobile to be located in a Rayleigh fading environment. Also, it assumes two antennas at the mobile, which are completely uncorrelated. The correlation between the wave patterns at the receiver, resulting from the two transmitted messages, is varied. The results are very promising. The BER falls off rapidly with decreasing envelope correlation between the two base station antennas. However, it does not fall off as rapidly as for the deterministic model. The stochastic model indicates that a practical system should work well both for the uplink and the downlink.

To extract the information from the measured data, a multivariable *Decision Feedback Equalizer* (DFE) has been derived and used. This DFE can be used for arbitrary numbers of measured signals (receivers) and messages (transmitters). For the case of one message and multiple antennas, this DFE is closely related to the maximal ratio combiner. Two other types of equalizer structures, the *Linear Feedback Equalizer* (LFE) and the *Viterbi algorithm* have been considered but deemed inappropriate as multivariable equalizers.

One important aspect, only mentioned very briefly, is that *overall system aspects must be taken into account when discussing possible capacity increases.* Some additional system capabilities must also be implemented. Today, switching *between* different cells is an administrative task performed by the supervisory system, but using the algorithms proposed in this thesis, an intelligent system of channel management *within* the cells must be devised as well.

To claim that the data rate can be doubled might be too optimistic. When more transmitters are added, the overall radio transmitter power in the cell is increased. This results in increased co-channel interference in neighboring cells, which will reduce the possibility for frequency reuse in other cells.

If the traffic load in the system is low temporarily, and the increased capacity is not needed for increasing the number of users, it is still possible to use the free capacity. For example, the data transmission rate could be doubled to increase the speech quality. It is simply a matter of splitting the double-rate transmission into two parts, and transmitting each part through a separate antenna.

Another possibility when the traffic load is low, is to use a multivariable DFE, with one message and two measured signals. This DFE has been simulated, and the BER which is achieved from it is extremely low, see Figure 5.9. In fact, *the BER is considerably lower than it is when any kind of conventional antenna diversity is used.*

6.2 Problems

The suggested new method provides new problems as well, not previously encountered. One is the carrier wave frequency. Recall that the basic idea was to reuse a frequency within one cell. This is all well, but what if the two carrier frequencies are not exactly equal? In the baseband, this will lead to rapidly changing channel coefficients. This is the same problem as the Doppler shift, that a mobile encounters as it is moving. In this case however, the problem could be an order of magnitude worse. In principle, it would, of course, be possible to improve the frequency stability of the oscillators in the telephones, but one reason for abandoning pure FDMA in the new digital systems, is that it is easier to manufacture accurate clocks than to manufacture accurate oscillators.

Another problem could be the sampling phase. The methods implicitly assume that the symbols from the two transmitters reach the receiver simultaneously.

This might be difficult to achieve, and if the symbols arrive asynchronously, either transmitter could possibly receive a very bad local SNR. See Figure 6.1. In this case, better synchronization would, of course, be beneficial.

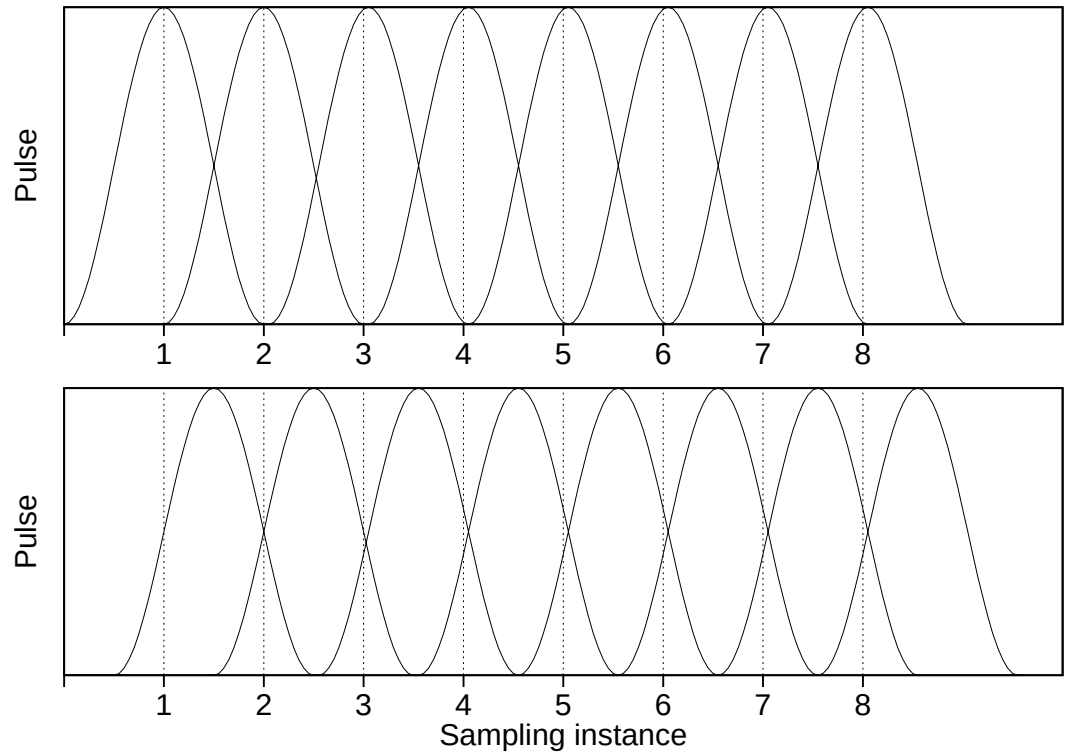

Figure 6.1: A problem with the sampling phase. Each graph shows one message. Each message is in this case a sequence of eight +1, pulse shaped with a raised cosine pulse. The sum of these two message is received at one antenna, and sampling is performed at the time instances marked by dotted, vertical lines. It is clearly seen that the sum of the two messages will mostly consist of the upper message; hence the SNR for the lower message is considerably lower.

6.3 Future work

As already mentioned, it is possible to generalize and investigate properties of IIR DFE's, colored noise and arbitrary numbers of messages and antennas.

If a hand-held mobile is assumed, the assumption of completely uncorrelated signals at the two antennas of the mobile, is probably hard to fulfill, at least for the present generation of systems. Relaxing the assumption of uncorrelated antennas at the mobile, and study the BER as a function of the correlation both at the transmitter *and* at the receiver is thus an interesting problem.

If the number of base station/mobile antennas were increased above two, how would this affect the performance? Is it possible to accommodate even more mobiles at one frequency, or is it better to increase the quality of the two transmis-

sions that are carried out? One can foresee an interesting possibility to combine the deterministic and the stochastic approach if four base station antennas were used. For instance, assume two pairs of antennas, separated by a long distance, sufficiently far apart so that the antenna pairs are *mutually* uncorrelated. The distance between the two antennas in each pair should however be short in order to get strongly correlated signals *within* each antenna pair. Each pair might be used as a directional antenna when transmitting. The message to one mobile is transmitted only (or at least mostly) in direction towards that mobile. Even if the effect of the directional antenna only partly works, and the other mobile is reached by the message intended for the first mobile, the "unwanted" message will be weaker. Hence, the directional effect will suppress the undesired signal at each mobile. This will probably lead to more errors for the undesired message, but less for the desired one, and hence result in higher overall performance.

Other aspects, which should always be considered when it comes to digital mobile radio communications, are the following three items:

- Identification of channels. How is the identification affected? The number of coefficients to estimate is increased by a factor of four in the proposed system, but the number of data points is only doubled. This is a problem.
- Tracking. If the channel coefficients vary considerably over a transmission period, they must be tracked.
- Robust design. Is it possible to cope with variations in the channel estimates without the equalization collapses?

These items have not been considered in the present thesis, and are obvious candidates for future research.

Bibliography

[1] A Ahlén and M Sternad, "Wiener filter design using polynomial equations," *IEEE Transactions on Signal Processing*, vol. 39, no. 11, pp. 2387–2399, November 1991.

[2] A Ahlén and M Sternad, "Derivation and design of Wiener filters using polynomial equations,", in C T Leondes, editor, *Stochastic Techniques in Digital Signal Processing*, pp. 353–418, Academic Press, New York, NY, 1994.

[3] L Ahlin and J Zander, *Digital radiokommunikation–system och metoder.* Lund, Sweden: Studentlitteratur, 1992, In Swedish.

[4] M Alonso and E Finn, *Fundamental University Physics; Fields and Waves.* Reading, MA: Addison–Wesley Publishing Company, 1983.

[5] P Balaban and J Salz, "Optimum diversity combining and equalization in digital data transmission with applications to cellular mobile radio - Part I: Theoretical considerations," *IEEE Transactions on Communications*, vol. 40, no. 5, pp. 885–894, 1992.

[6] P Balaban and J Salz, "Optimum diversity combining and equalization in digital data transmission with applications to cellular mobile radio - Part II: Numerical results," *IEEE Transactions on Communications*, vol. 40, no. 5, pp. 895–907, May 1992.

[7] R V Churchill and J W Brown, *Complex Variables and Applications.* Singapore, Republic of Singapore: McGraw–Hill, 1984.

[8] K Giridar, S Chari, J Shynk and R Gooch, "Joint demodulation of co-channel signals using MLSE and MAPSD algorithms," in *Proceedings of ICASSP*, vol. 4, Minneapolis, April 1993, pp. 160–163.

[9] W C Jakes, editor, *Microwave Mobile Communications.* New York, NY: Wiley, 1974.

[10] W Lee, *Mobile Communications Engineering.* New York, NY: McGraw–Hill, 1982.

[11] W Lee, *Mobile Communications Design Fundamentals.* New York, NY: McGraw–Hill, 1986.

[12] L Lindbom, *Adaptive Equalization for Fading Mobile Radio Channels.* Licentiate thesis, Department of Technology, Uppsala University, Uppsala, Sweden, November 1992.

[13] J G Proakis, *Digital Communications*. New York, NY: McGraw–Hill, 1984.

[14] L Råde and B Westergren, *Mathematics Handbook*. Lund, Sweden: Studentlitteratur, 1988.

[15] M R Spiegel, *Mathematical Handbook*. New York, NY: McGraw–Hill, 1968.

[16] M Sternad and A Ahlén, "The structure and design of realizable decision feedback equalizers for IIR channels with coloured noise," *IEEE Transactions on Information Theory*, vol. 36, no. 4, pp. 848–858, July 1990.

[17] M Sternad, A Ahlén and E Lindskog, "Robust decision feedback equalizers," in *Proceedings of ICASSP*, vol. 3, Minneapolis, April 1993, pp. 555–558.

Appendix A

Rayleigh fading

Consider the following situation:

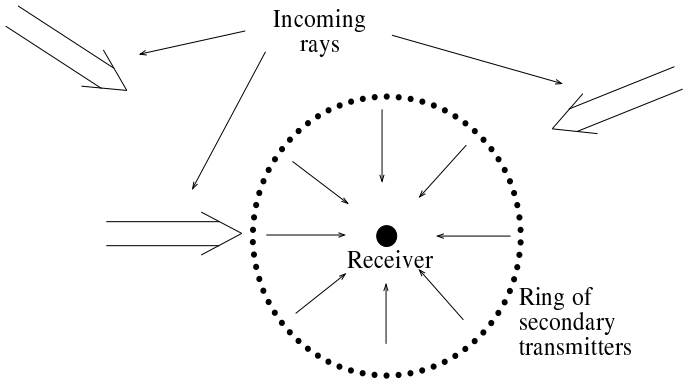

Figure A.1: Very many (N) scatterers surround the mobile. Each dot is considered to be a secondary transmitter. The large arrows are reflexes, resulting in intersymbol interference. The mobile is presumed to be located in the middle of a circle of secondary transmitters.

In reality, the transmitters are of course not located exactly on a circle. Since we are only going to make a statistical analysis of the problem, this does not matter. This is because the phase shift contributed by each secondary transmitter is *unknown*, and only its statistical distribution is known. Suppose the damping and phase shift contributed by the jth transmitter are a_j^0 and ψ_j^0, respectively. This can be replaced by an *equivalent* damping and phase shift at the antenna, a_j and ψ_j, respectively. These equivalent random variables are discussed. Hence, the contribution at the antenna from the jth secondary transmitter is $a_j e^{j\psi_j}$. The distribution of a_j is unknown, but its mean power is

$$E[a_j^2] = \frac{2\sigma_b^2}{N} \ .$$

The distribution of ψ_j is uniform in $[0, 2\pi]$:

$$\psi_j \in U[0, 2\pi] \ .$$

Making the assumptions made in subsection 2.2.3, we obtain the following expression for the channel coefficient:

$$b = \lim_{N\to\infty} \sum_{i=1}^{N} a_i e^{\jmath\psi_i} \ .$$

This is true for every channel coefficient. For simplicity, the subscript k has been dropped.

According to the central limit theorem, the sum of an infinite number of identically distributed random variables is Gaussian distributed. Hence, it follows at once that

$$b^r, b^i \in \mathcal{N}[0, \sigma_b] \ .$$

Now consider two closely spaced antennas in the center of the circle of Figure A.1. Figure A.2 shows a magnification of the center, depicting the incoming ray from one of the scatterers. Using antenna 1 as the reference, the channels associated

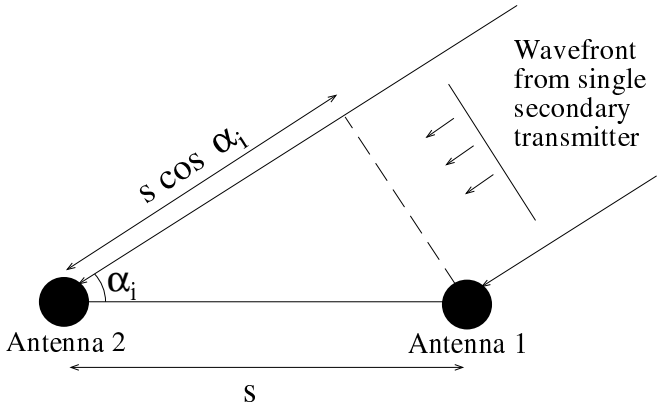

Figure A.2: A magnification of the center of Figure A.1.

with the two antennas can be written as

$$b(0) = \lim_{N\to\infty} \sum_{i=1}^{N} a_i e^{\jmath\psi_i} \tag{A.1}$$

$$b(x) = \lim_{N\to\infty} \sum_{i=1}^{N} a_i e^{\jmath(\psi_i + x\cos\alpha_i)} \tag{A.2}$$

where

$$x \triangleq \frac{2\pi s}{\lambda} \ .$$

Splitting these equations into real and imaginary parts yields

$$b^r(x) = \lim_{N\to\infty} \sum_{i=1}^{N} a_i[\Delta x_i(x)\cos\psi_i - \Delta y_i(x)\sin\psi_i] \tag{A.3}$$

$$b^i(x) = \lim_{N\to\infty} \sum_{i=1}^{N} a_i[\Delta y_i(x)\cos\psi_i + \Delta x_i(x)\sin\psi_i] \tag{A.4}$$

$$\Delta x_i(x) = \cos(x\cos\alpha_i) \quad \Delta y_i(x) = \sin(x\cos\alpha_i) \ .$$

Equations (A.3) and (A.4) can be rewritten

$$\begin{aligned} \underline{b}_{ri}(x) &= \begin{pmatrix} b^r(x) \\ b^i(x) \end{pmatrix} = \lim_{N\to\infty} \sum_{i=1}^{N} a_i \begin{pmatrix} \Delta x_i(x) & -\Delta y_i(x) \\ \Delta y_i(x) & \Delta x_i(x) \end{pmatrix} \begin{pmatrix} \cos\psi_i \\ \sin\psi_i \end{pmatrix} \\ &= \lim_{N\to\infty} \sum_{i=1}^{N} a_i \Delta \begin{pmatrix} \cos\psi_i \\ \sin\psi_i \end{pmatrix} \ . \end{aligned}$$

The expectation of $\underline{b}_{ri}(x)$ is obviously zero, since the expectation of both $\sin\psi_i$ and $\cos\psi_i$ is zero. Hence the covariance of $\underline{b}_{ri}(x)$ can be written

$$\mathbf{R}(\xi) = E[\underline{b}_{ri}(x)\underline{b}_{ri}^T(x-\xi)] = E \begin{pmatrix} b^r(x)b^r(x-\xi) & b^r(x)b^i(x-\xi) \\ b^i(x)b^r(x-\xi) & b^i(x)b^i(x-\xi) \end{pmatrix} \ .$$

Using (A.3) and (A.4), the covariance function can be rewritten

$$\mathbf{R}(\xi) = \lim_{N\to\infty} E \sum_{j=1}^{N}\sum_{k=1}^{N} a_j a_k \Delta \begin{pmatrix} \cos\psi_j\cos\psi_k & \cos\psi_j\sin\psi_k \\ \sin\psi_j\cos\psi_k & \sin\psi_j\sin\psi_k \end{pmatrix} \Delta^T . \qquad (A.5)$$

Moving the expectation operator inside the summation and using

$$E[\cos\psi_j \sin\psi_k] = 0$$

$$E[\cos\psi_j\cos\psi_k] = E[\sin\psi_j\sin\psi_k] = \frac{\delta_{jk}}{2}$$

$$E[a_j^2] = \frac{2\sigma_b^2}{N}$$

yields

$$\mathbf{R}(\xi) = \lim_{N\to\infty} \frac{2\sigma_b^2}{N} \sum_{j=1}^{N} \Delta \begin{pmatrix} \frac{1}{2} & 0 \\ 0 & \frac{1}{2} \end{pmatrix} \Delta^T = \lim_{N\to\infty} \frac{\sigma_b^2}{N} \sum_{j=1}^{N} \Delta\Delta^T \ . \qquad (A.6)$$

Performing the matrix multiplication gives matrix elements which look like

$$\begin{aligned} \Delta_{jk} &= \pm\Delta x_j(x)\Delta x_j(x-\xi) \pm \Delta y_j(x)\Delta y_j(x-\xi) \qquad (A.7) \\ &= \pm\cos(x\cos\alpha_i)\cos((x-\xi)\cos\alpha_i) \pm \sin(x\cos\alpha_i)\sin((x-\xi)\cos\alpha_i) \ . \end{aligned}$$

Using familiar trigonometric identities on (A.7) gives

$$\begin{aligned} \mathbf{R}(\xi) &= \frac{\sigma_b^2}{N} \lim_{N\to\infty} \sum_{j=1}^{N} \begin{pmatrix} \cos(\xi\cos\alpha_i) & -\sin(\xi\cos\alpha_i) \\ \sin(\xi\cos\alpha_i) & \cos(\xi\cos\alpha_i) \end{pmatrix} \\ &= \sigma_b^2 \lim_{N\to\infty} \begin{pmatrix} \frac{1}{N}\sum_{j=1}^{N}\cos(\xi\cos\alpha_i) & \frac{1}{N}\sum_{j=1}^{N} -\sin(\xi\cos\alpha_i) \\ \frac{1}{N}\sum_{j=1}^{N}\sin(\xi\cos\alpha_i) & \frac{1}{N}\sum_{j=1}^{N}\cos(\xi\cos\alpha_i) \end{pmatrix} \ . \qquad (A.8) \end{aligned}$$

Now, since $\alpha_i = \frac{2\pi i}{N}$, it is possible to use the usual equality between a Riemann sum and an integral:

$$\lim_{N\to\infty} \frac{1}{N} \sum_{i=1}^{N} f(a + \frac{b-a}{N} i) = \frac{1}{b-a} \int_a^b f(x)dx \ .$$

Using this equality on each of the matrix elements in (A.8) yields

$$\begin{aligned}\mathbf{R}(\xi) &= \frac{\sigma_b^2}{2\pi}\begin{pmatrix} \int_0^{2\pi}\cos(\xi\cos\alpha)d\alpha & -\int_0^{2\pi}\sin(\xi\cos\alpha)d\alpha \\ \int_0^{2\pi}\sin(\xi\cos\alpha)d\alpha & \int_0^{2\pi}\cos(\xi\cos\alpha)d\alpha \end{pmatrix} \\ &= \sigma_b^2\begin{pmatrix} J_0(\xi) & 0 \\ 0 & J_0(\xi) \end{pmatrix}\end{aligned}$$

where the final equality follows from the integral representation of Bessel functions.

Appendix B

Calculation of the verification formula

In the simplest case of a one tap channel using the deterministic model, the channel is described by

$$\begin{aligned} \underline{y}(t) &= \begin{pmatrix} y_1(t) \\ y_2(t) \end{pmatrix} = \begin{pmatrix} 1 & 1 \\ e^{-\jmath\psi_1} & e^{-\jmath\psi_2} \end{pmatrix} \begin{pmatrix} d_1(t) \\ d_2(t) \end{pmatrix} + \begin{pmatrix} v_1(t) \\ v_2(t) \end{pmatrix} \qquad \text{(B.1)} \\ &= \mathbf{B}\underline{d}(t) + \underline{v}(t) \end{aligned}$$

where

$$d_i(t) \in \{-1, 1\} \quad i = 1, 2 \qquad \underline{v}(t) \in \mathcal{CN}(0, \mathbf{I}) \; .$$

Since there is only one tap in the channel, there is no intersymbol interference, and hence, no need for the Q filter in the DFE. The only remaining part of the equalizer is the prefilter. The smoothing lag and hence the order of the prefilter is chosen to be zero, since there is no need to collect signal energy in later sampling intervals. The equalizing then gives the estimate

$$\hat{\underline{d}}(t) = \mathbf{S}\underline{y}(t) = \mathbf{SB}\underline{d}(t) + \mathbf{S}\underline{v}(t)$$

and the estimation error $\underline{z}(t)$ is given by

$$\underline{z}(t) = \underline{d}(t) - \hat{\underline{d}}(t) = \underbrace{(\mathbf{I} - \mathbf{SB})\underline{d}(t)}_{\underline{z}^{(1)}(t)} + \underbrace{\mathbf{S}\underline{v}(t)}_{\underline{z}^{(2)}(t)} \; . \qquad \text{(B.2)}$$

In (B.2), $\underline{z}^{(1)}(t)$ is due to incomplete channel inversion, and $\underline{z}^{(2)}(t)$ is due to the noise. The decisioned symbol is denoted $\overline{\underline{d}}(t) = (\overline{d}_1(t)\ \overline{d}_2(t))^T$.

The equalizer matrix $\mathbf{S}$ is most easily calculated using the method of completing the squares. This gives

$$\mathbf{S} = \mathbf{B}^*(\mathbf{BB}^* + E[\underline{v}(t)\underline{v}^*(t)])^{-1} = \mathbf{B}^*(\mathbf{BB}^* + \mathbf{I})^{-1} \; . \qquad \text{(B.3)}$$

If (B.1) is inserted into (B.3), $\mathbf{S}$ becomes

$$\mathbf{S} = \frac{1}{6 - 2\cos\Delta\varphi} \begin{pmatrix} 2 - e^{\jmath\Delta\varphi} & e^{\jmath\varphi_1}(2 - e^{-\jmath\Delta\varphi}) \\ 2 - e^{-\jmath\Delta\varphi} & e^{\jmath\varphi_2}(2 - e^{\jmath\Delta\varphi}) \end{pmatrix}$$

and $(\mathbf{I}-\mathbf{SB})$ becomes

$$(\mathbf{I}-\mathbf{SB}) = \frac{1}{6-2\cos\Delta\varphi}\begin{pmatrix} 2 & -(1+e^{\jmath\Delta\varphi}) \\ -(1+e^{-\jmath\Delta\varphi}) & 2 \end{pmatrix} .$$

The probability density function for the noise component of the error, $\underline{z}^{(2)}(t)$, is given by

$$p(\underline{z}^{(2)}(t)) = \frac{1}{\pi^2 \det\Lambda} e^{-(\underline{z}^{(2)})^*(t)\Lambda^{-1}\underline{z}^{(2)}(t)} \tag{B.4}$$

where

$$\Lambda = E[\underline{z}^{(2)}(t)\underline{z}^{(2)*}(t)] = \mathbf{SS}^* = \frac{1}{(6-2\cos\Delta\varphi)^2}\begin{pmatrix} 10-8\cos\Delta\varphi & e^{2\jmath\Delta\varphi}+e^{-\jmath\Delta\varphi} \\ e^{-2\jmath\Delta\varphi}+e^{\jmath\Delta\varphi} & 10-8\cos\Delta\varphi \end{pmatrix} .$$

If $\underline{z}^{(2)}(t) = (x_1+\jmath y_1 \;\; x_2+\jmath y_2)^T$, the expression (B.4) can be written

$$p(\underline{z}^{(2)}(t)) = \frac{1}{\pi^2 \det\Lambda} e^{g(x_1,x_2,y_1,y_2)} \tag{B.5}$$

with

$$g(x_1,x_2,y_1,y_2) = k_1[k_2(x_1x_2+y_1y_2)+k_3(x_1y_2-x_2y_1)-k_4(x_1^2+x_2^2+y_1^2+y_2^2)]$$

where

$$k_1 = \frac{4(3-\cos\Delta\varphi)^2}{49-77\cos\Delta\varphi+32\cos^2\Delta\varphi-4\cos^3\Delta\varphi} \tag{B.6}$$

$$k_2 = \cos 2\Delta\varphi+\cos\Delta\varphi \tag{B.7}$$

$$k_3 = \sin 2\Delta\varphi-\sin\Delta\varphi \tag{B.8}$$

$$k_4 = 5-4\cos\Delta\varphi\ . \tag{B.9}$$

Also,

$$\det\Lambda = \frac{2}{k_1(6-2\cos\Delta\varphi)^2} .$$

How large is the probability to make an erroneous decision? The probability is definitely depending on what symbols were transmitted. First suppose $\underline{d}(t) = (1\ 1)^T$. The probability that the decisioned symbol $\overline{d_1}(t)$ differs from $d_1(t)$ is the probability that

$$\mathrm{Re}(\hat{d}_1(t)) < 0 \Leftrightarrow \mathrm{Re}(z_1(t)) > 1 \Leftrightarrow \mathrm{Re}(z_1^{(1)}(t)+z_1^{(2)}(t)) > 1$$

$$\Updownarrow$$

$$\mathrm{Re}(z_1^{(2)}(t)) > 1-\mathrm{Re}(z_1^{(1)}(t)) .$$

The real part of $\underline{z}^{(1)}(t)$ can be calculated through

$$\mathrm{Re}[(\mathbf{I}-\mathbf{SB})\underline{d}(t)] = \mathrm{Re}[(\mathbf{I}-\mathbf{SB})]\underline{d}(t) . \tag{B.10}$$

This gives for $\underline{d}(t) = (1\ 1)^T$

$$\mathrm{Re}(z_1^{(1)}(t)) = \frac{1-\cos\Delta\varphi}{6-2\cos\Delta\varphi}$$

and for an erroneous decision to happen, the following must happen:

$$\mathrm{Re}(z_1^{(2)}(t)) > \frac{5-\cos\Delta\varphi}{6-2\cos\Delta\varphi} \triangleq \delta_1 \ .$$

The probability can then be written using (B.5):

$$\begin{aligned} P_{wrong}(\Delta\varphi) &= P(\mathrm{Re}(z_1^{(2)}(t)) > \delta_1) \\ &= \frac{1}{\pi^2 \det\Lambda} \int_{\delta_1}^{\infty}\int_{-\infty}^{\infty}\int_{-\infty}^{\infty}\int_{-\infty}^{\infty} e^{g(x_1,x_2,y_1,y_2)} dy_2 dy_1 dx_2 dx_1 \ . \end{aligned}$$

Due to the symmetry of the problem, the probability that $\overline{d_2}(t)$ differs from $d_2(t)$ is given by the integral

$$\begin{aligned} P_{wrong}(\Delta\varphi) &= P(\mathrm{Re}(z_2^{(2)}) > \delta_1) \\ &= \frac{1}{\pi^2 \det\Lambda} \int_{\delta_1}^{\infty}\int_{-\infty}^{\infty}\int_{-\infty}^{\infty}\int_{-\infty}^{\infty} e^{g(x_1,x_2,y_1,y_2)} dy_2 dy_1 dx_1 dx_2 \ . \end{aligned} \quad \text{(B.11)}$$

When $\underline{d}(t) = (-1 \ \ -1)^T$, the probabilities are the same, also from symmetry. The situation is a bit different when $\underline{d}(t) = (1 \ \ -1)^T$, however. The condition for an erroneous estimation of d_1 is still the same:

$$\mathrm{Re}(\hat{d}_1(t)) < 0 \Leftrightarrow \mathrm{Re}(z_1(t)) > 1 \Leftrightarrow \mathrm{Re}(z_1^{(1)}(t) + z_1^{(2)}(t)) > 1$$

$$\Updownarrow$$

$$\mathrm{Re}(z_1^{(2)}(t)) > 1 - \mathrm{Re}(z_1^{(1)}(t)) \ .$$

When $\mathrm{Re}(z_1^{(1)}(t))$ is calculated from (B.10), the following limit is obtained:

$$\mathrm{Re}(z_1^{(1)}(t)) = \frac{3-3\cos\Delta\varphi}{6-2\cos\Delta\varphi} \triangleq \delta_2 \ .$$

The probability of error is then

$$\begin{aligned} P_{wrong}(\Delta\varphi) &= P(\mathrm{Re}(z_1^{(2)}(t)) > \delta_2) \\ &= \frac{1}{\pi^2 \det\Lambda} \int_{\delta_2}^{\infty}\int_{-\infty}^{\infty}\int_{-\infty}^{\infty}\int_{-\infty}^{\infty} e^{g(x_1,x_2,y_1,y_2)} dy_2 dy_1 dx_2 dx_1 \end{aligned} \quad \text{(B.12)}$$

where symmetry again can be applied, so that the probability for error in $d_2(t)$ is the same. Using symmetry a fourth time, it is concluded that the probabilities are the same if the transmitted symbols are $\underline{d}(t) = (-1 \ \ 1)^T$.

The problem has thus been reduced to the calculation of the integrals in (B.11) and (B.12). Study the integral in (B.11). It can be written

$$\begin{aligned} P_{wrong}(\Delta\varphi) &= \frac{1}{\pi^2 \det\Lambda} \int_{\delta_1}^{\infty} e^{-k_1k_4x_1^2} \int_{-\infty}^{\infty} e^{-k_1k_4x_2^2 + k_1k_2x_1x_2} \\ &\quad \times \int_{-\infty}^{\infty} e^{-k_1k_4y_1^2 - k_1k_3x_2y_1} \int_{-\infty}^{\infty} e^{-k_1k_4y_2^2 + k_1k_3x_1y_2 + k_1k_2y_1y_2} dy_2 dy_1 dx_2 dx_1 \ . \end{aligned}$$

Study the exponent in the innermost integrand:

$$g_1(y_2) = -k_1k_4y_2^2 + k_1k_3x_1y_2 + k_1k_2y_1y_2 \ .$$

Now, completing the squares gives

$$\begin{aligned} g_1(y_2) &= -k_1k_4(y_2^2 - \frac{k_3}{k_4}x_1y_2 - \frac{k_2}{k_4}y_1y_2) = -k_1k_4(y_2^2 - \underbrace{(\frac{k_3}{k_4}x_1 + \frac{k_2}{k_4}y_1)}_{a}y_2) \\ &= -k_1k_4(y_2^2 - ay_2 + \frac{a^2}{4}) + \frac{k_1k_4a^2}{4} \\ &= -k_1k_4(y_2 - \frac{a}{2})^2 + \frac{k_1k_4a^2}{4} \ . \end{aligned}$$

Hence the innermost integral can be written:

$$I_1 = e^{\frac{k_1k_4a^2}{4}} \int_{-\infty}^{\infty} e^{-k_1k_4(y_2-\frac{a}{2})^2} dy_2 = e^{\frac{k_1k_4a^2}{4}} \sqrt{\frac{\pi}{k_1k_4}} \ . \tag{B.13}$$

The last equality can be found in any collection of formulas. Move the constant in front of the entire integral, but insert $e^{\frac{k_1k_4a^2}{4}}$ into the second innermost integral. It can then be written

$$I_2 = \int_{-\infty}^{\infty} e^{(\frac{k_1k_4a^2}{4} - k_1k_4y_1^2 - k_1k_3x_2y_1)} dy_1 \ . \tag{B.14}$$

In the same way, complete the squares in the exponent in the integrand in (B.14):

$$\begin{aligned} g_2(y_1) &= -k_1k_4y_1^2 - k_1k_3x_2y_1 + \frac{k_1k_4}{4}(\frac{k_3}{k_4}x_1 + \frac{k_2}{k_4}y_1)^2 \\ &= k_1[-k_4y_1^2 - k_3x_2y_1 + \frac{1}{4k_4}(k_3^2x_1^2 + 2k_2k_3x_1y_1 + k_2^2y_1^2)] \\ &= k_1[\underbrace{-(k_4 - \frac{k_2^2}{4k_4})}_{a_1 \geq 0} + \underbrace{(-k_3x_2 + \frac{k_2k_3}{2k_4}x_1)}_{a_2} y_1 + \frac{k_3^2}{4k_4}x_1^2] \\ &= a_1k_1[-y_1^2 + \frac{a_2}{a_1}y_1 + \frac{k_3^2x_1^2}{4k_4a_1}] \\ &= a_1k_1[-(y_1 - \frac{a_2}{2a_1})^2 + a_1k_1(\frac{k_3^2x_1^2}{4k_4a_1} + (\frac{a_2}{2a_1})^2)] \ . \end{aligned}$$

Hence I_2 can be written

$$\begin{aligned} I_2 &= e^{a_1k_1(\frac{k_3^2x_1^2}{4k_4a_1} + (\frac{a_2}{2a_1})^2)} \int_{-\infty}^{\infty} e^{-(y_1 - \frac{a_2}{2a_1})^2} dy_1 \\ &= e^{a_1k_1(\frac{k_3^2x_1^2}{4k_4a_1} + (\frac{a_2}{2a_1})^2)} \sqrt{\frac{\pi}{a_1k_1}} \ . \end{aligned} \tag{B.15}$$

Proceeding as before gives the exponent of the second outermost integrand:

$$g_3(x_2) = -k_1a_3(x_2 - \frac{a_4}{2a_3})^2 + \frac{k_1k_3^2x_1^2}{4k_4}(\frac{k_2^2}{4a_1k_4} + 1) + \frac{k_1a_4^2}{4a_3}$$

where

$$\begin{aligned} a_3 &= k_4 - \frac{k_3^2}{4a_1} \geq 0 \\ a_4 &= k_2x_1(1 - \frac{k_3^2}{4a_1k_4}) \ . \end{aligned}$$

This results in

$$
\begin{aligned}
I_3 &= e^{\frac{k_1 k_3^2 x_1^2}{4k_4}(\frac{k_2^2}{4a_1 k_4}+1)+\frac{k_1 a_4^2}{4a_3}} \int_{-\infty}^{\infty} e^{-k_1 a_3 (x_2 - \frac{a_4}{2a_3})^2} \\
&= e^{\frac{k_1 k_3^2 x_1^2}{4k_4}(\frac{k_2^2}{4a_1 k_4}+1)+\frac{k_1 a_4^2}{4a_3}} \sqrt{\frac{\pi}{k_1 a_3}} \ . \qquad \text{(B.16)}
\end{aligned}
$$

Using the constants obtained in (B.13), (B.15) and (B.16) and the integrand from (B.16) gives

$$
P_{wrong}(\Delta\varphi) = \frac{1}{\sqrt{\pi}\sqrt{k_1^3 k_4 a_1 a_3} \det \Lambda} \int_{\delta_1}^{\infty} e^{\frac{k_1 a_4^2}{4a_3}} e^{-k_1 [k_4 - \frac{k_3^2}{4k_4}(\frac{k_2^2}{4a_1 k_4}+1)]} dx_1 \ .
$$

For the last time, complete the squares in the exponent in the integrand. This gives

$$
\begin{aligned}
P_{wrong}(\Delta\varphi) &= \frac{1}{\sqrt{\pi}\sqrt{k_1^3 k_4 a_1 a_3} \det \Lambda} \int_{\delta_1}^{\infty} e^{-\frac{k_1 a_1 a_3}{k_4} x_1^2} dx_1 \\
&= \frac{(6 - 2\cos\Delta\varphi)^2}{2\sqrt{\pi}\sqrt{k_1 k_4 a_1 a_3}} \int_{\delta_1}^{\infty} e^{-\frac{k_1 a_1 a_3}{k_4} x_1^2} dx_1 \\
&= \frac{(6 - 2\cos\Delta\varphi)^2}{2\sqrt{\pi}\sqrt{k_1 k_4 a_1 a_3}} \int_{\delta_1}^{\infty} e^{-\frac{k_1 a_1 a_3}{k_4} x_1^2} dx_1 \\
&= \frac{(6 - 2\cos\Delta\varphi)^2}{2\sqrt{\pi}\sqrt{k_1 k_4 a_1 a_3}} \sqrt{\frac{k_4}{k_1 a_1 a_3}} \int_{\delta_1'}^{\infty} e^{-t^2} dt \\
&= \frac{(6 - 2\cos\Delta\varphi)^2}{2\sqrt{\pi} k_1 a_1 a_3} \int_{\delta_1'}^{\infty} e^{-t^2} dt \\
&= \frac{1}{\sqrt{\pi}} \int_{\delta_1'}^{\infty} e^{-t^2} dt \qquad \text{(B.17)}
\end{aligned}
$$

where

$$
\delta_1' \triangleq \delta_1 \sqrt{\frac{k_1 a_1 a_3}{k_4}} \ .
$$

The last equality in (B.17) follows from the expressions for k_1, a_1 and a_3. Finally, δ_1' can be simplified to

$$
\delta_1' = \frac{5 - \cos\Delta\varphi}{\sqrt{10 - 8\cos\Delta\varphi}} \ . \qquad \text{(B.18)}
$$

The calculations for (B.12) are completely analogous. In this case, the result is

$$
P_{wrong}(\Delta\varphi) = \frac{1}{\sqrt{\pi}} \int_{\delta_2'}^{\infty} e^{-t^2} dt \qquad \text{(B.19)}
$$

where

$$
\delta_2' \triangleq \frac{3 - 3\cos\Delta\varphi}{\sqrt{10 - 8\cos\Delta\varphi}} \ . \qquad \text{(B.20)}
$$

The total BER which will be achieved in the simulations is the mean of these two probabilities. This is again concluded because of the symmetry. Equation (B.17) and (B.19) together with (B.18) and (B.20) constitute the verification formula (5.2).

Appendix C

Derivation of multivariable DFE

The problem is the following: given a FIR channel of order n

$$\underline{y}(t) = \boldsymbol{B}(q^{-1})\underline{d}(t) + \underline{v}(t) \tag{C.1}$$

$$E[\underline{d}(t)\underline{d}^*(\tau)] = \delta_{t\tau}\mathbf{I}_{n_d} \qquad E[\underline{v}(t)\underline{v}^*(\tau)] = \delta_{t\tau}\Psi \qquad E[\underline{v}(t)\underline{d}^*(\tau)] = \mathbf{0}$$

where the dimensions of the channel matrix coefficients are

$$\mathbf{B}_k = \underbrace{\begin{pmatrix} & \bullet & \end{pmatrix}}_{n_d} \Bigg\} n_y$$

and a FIR DFE

$$\underline{\hat{d}}(t) = q^{m_f}\boldsymbol{S}(q^{-1})\underline{y}(t) - \boldsymbol{Q}(q^{-1})\overline{\underline{d}}(t-1) \tag{C.2}$$

with matrix filter coefficients of dimensions

$$\mathbf{S}_k = \underbrace{\begin{pmatrix} & \bullet & \end{pmatrix}}_{n_y} \Bigg\} n_d \qquad \mathbf{Q}_k = \underbrace{\begin{pmatrix} & \bullet & \end{pmatrix}}_{n_d} \Bigg\} n_d \ ,$$

calculate the polynomial matrices so that the MSE of the filtering error

$$\underline{z}(t) = \underline{d}(t) - \underline{\hat{d}}(t) \tag{C.3}$$

is minimized. Assume correct past decisions, i.e.

$$\overline{\underline{d}}(t) = \underline{d}(t) \ . \tag{C.4}$$

This means calculating the probability of the *first* error. After the first error has occurred, the probability of error in the next symbol increases substantially. This is ignored, however.

Inserting (C.1), (C.2) and (C.4) into (C.3) yields

$$\begin{aligned} \underline{z}(t-m_f) &= \underline{d}(t-m_f) - q^{m_f}\boldsymbol{S}(q^{-1})\boldsymbol{B}(q^{-1})\underline{d}(t-m_f) + \\ &+ \boldsymbol{Q}(q^{-1})\underline{d}(t-m_f-1) - \boldsymbol{S}(q^{-1})\underline{v}(t-m_f) \ . \end{aligned} \tag{C.5}$$

In order to minimize $E[|\underline{z}(t)|^2]$, we adopt the variational scheme, suggested in [1], see also [2] and [16]. Introduce an arbitrary variation of the estimation error (C.5), given by a linear combination of the signals we are allowed to base our estimate on, at time $t - m_f$:

$$\underline{n}(t) = \underline{n_1}(t) + \underline{n_2}(t) = \boldsymbol{G}_1(q^{-1})\underline{y}(t) + q^{-m_f-1}\boldsymbol{G}_2(q^{-1})\underline{d}(t)$$

where $\boldsymbol{G}_1(q^{-1})$ and $\boldsymbol{G}_2(q^{-1})$ are arbitrary, stable, multivariable filters of appropriate dimensions.

If orthogonality between the estimation error (C.5) and $\underline{n_1}(t)$ and $\underline{n_2}(t)$ separately could be achieved, any variation $\underline{n}(t)$ is orthogonal to the filtering error (C.5), and hence (C.5) would be the smallest possible error. Our first aim is thus to prove that the following matrix is equal to zero:

$$E[\underline{z}(t-m_f)\underline{n}_1^*(t)] =$$

$$= E[\{(q^{-m_f}\mathbf{I}_{n_d} - \boldsymbol{S}(q^{-1})\boldsymbol{B}(q^{-1}) + q^{-m_f-1}\boldsymbol{Q}(q^{-1}))\underline{d}(t) - \boldsymbol{S}(q^{-1})\underline{v}(t)\} \times$$

$$\times \{\boldsymbol{G}_1(q^{-1})(\boldsymbol{B}(q^{-1})\underline{d}(t) + \underline{v}(t)\}^*] =$$

$$= \frac{1}{2\pi\jmath}\oint_{|z|=1}\{[z^{-m_f}\mathbf{I}_{n_d} - \boldsymbol{S}(z^{-1})\boldsymbol{B}(z^{-1}) + z^{-m_f-1}\boldsymbol{Q}(z^{-1})]\boldsymbol{I}_{n_d}\boldsymbol{B}_*(z) - \boldsymbol{S}(z^{-1})\Psi\}\boldsymbol{G}_{1*}(z)\frac{dz}{z}\,.$$

In the last equality, Parseval's relation has been used. It was also utilized that $E[\underline{v}(t)\underline{d}^*(\tau)] = 0$. According to Cauchy-Goursats theorem, the integral is zero if and only if the integrand is analytic within and on the unit circle. This is the case if each element of the integrand can be expressed as a polynomial in z. The condition for analyticity and hence orthogonality can thus be written:

$$\frac{[z^{-m_f}\mathbf{I}_{n_d} - \boldsymbol{S}(z^{-1})\boldsymbol{B}(z^{-1}) + z^{-m_f-1}\boldsymbol{Q}(z^{-1})]\boldsymbol{B}_*(z) - \boldsymbol{S}(z^{-1})\Psi}{z} = \boldsymbol{L}_{2*}(z)$$

$$\Updownarrow$$

$$[z^{-m_f}\mathbf{I}_{n_d} - \boldsymbol{S}(z^{-1})\boldsymbol{B}(z^{-1}) + z^{-m_f-1}\boldsymbol{Q}(z^{-1})]\boldsymbol{B}_*(z) - \boldsymbol{S}(z^{-1})\Psi = z\boldsymbol{L}_{2*}(z)\ . \quad \text{(C.6)}$$

for some matrix polynomial $\boldsymbol{L}_{2*}(z)$ of dimension $n_d|n_y$. Next, orthogonality with respect to $\underline{n_2}(t)$ is assured, which leads to the following result:

$$z\mathbf{I}_{n_d} - z^{m_f+1}\boldsymbol{S}(z^{-1})\boldsymbol{B}(z^{-1}) + \boldsymbol{Q}(z^{-1}) = z\boldsymbol{L}_{1*}(z) \qquad \text{(C.7)}$$

where L_{1*} is of dimension $n_d|n_d$. Multiply (C.7) with $z^{-m_f-1}\boldsymbol{B}_*(z)$ from the right, and subtract the result from (C.6). This gives

$$z^{-m_f}\boldsymbol{L}_{1*}(z)\boldsymbol{B}_*(z) - z\boldsymbol{L}_{2*}(z) = \boldsymbol{S}(z^{-1})\Psi\ . \qquad \text{(C.8)}$$

An intermediate result is obtained by multiplying (C.7) with z^{-1} and rearranging (C.8) :

$$\boldsymbol{I}_{n_d} + z^{-1}\boldsymbol{Q}(z^{-1}) = \boldsymbol{S}(z^{-1})z^{m_f}\boldsymbol{B}(z^{-1}) + \boldsymbol{L}_{1*}(z) \qquad \text{(C.9)}$$

$$z\boldsymbol{L}_{2*}(z) = -\boldsymbol{S}(z^{-1})\Psi + z^{-m_f}\boldsymbol{L}_{1*}(z)\boldsymbol{B}_*(z)\ . \tag{C.10}$$

This is a system of two coupled matrix polynomial Diophantine equations, with four unknown matrix polynomials, $\boldsymbol{Q}(z^{-1})$, $\boldsymbol{S}(z^{-1})$, $\boldsymbol{L}_{1*}(z)$, $\boldsymbol{L}_{2*}(z)$. To obtain a unique solution, the degrees of the respective polynomials must be

$$n_S = n_{L_1} = m_f \qquad\qquad n_Q = n_{L_2} = n-1\ .$$

As it stands, this system is difficult to solve, because of the large number of unknown matrices. However, by converting both equations into linear systems of equations in the coefficient matrices, and combining some of the equations from (C.9) with some of the equations from (C.10), a uniquely solvable system is obtained.

To convert (C.9) and (C.10) into a system of linear equations, write out the transpose of the equations for the powers z^0 to z^{m_f} from (C.9):

$$\begin{aligned}
z^0 :\ & \mathbf{I}_{n_d} &&= \mathbf{B}_0^T\mathbf{S}_{m_f}^T + \mathbf{B}_1^T\mathbf{S}_{m_f-1}^T + \ldots + \mathbf{B}_{n_b-m_f}^T\mathbf{S}_0^T + \overline{\mathbf{L}}_{10}\\
z^1 :\ & \mathbf{0} &&= \mathbf{B}_0^T\mathbf{S}_{m_f-1}^T + \mathbf{B}_1^T\mathbf{S}_{m_f-2}^T + \ldots + \mathbf{B}_{n_b-m_f-1}^T\mathbf{S}_0^T + \overline{\mathbf{L}}_{11}\\
\vdots\ :\ & \vdots && \qquad\vdots\\
z^{m_f-1} :\ & \mathbf{0} &&= \mathbf{B}_0^T\mathbf{S}_1^T + \mathbf{B}_1^T\mathbf{S}_0^T + \overline{\mathbf{L}}_{1(m_f-1)}\\
z^{m_f} :\ & \mathbf{0} &&= \mathbf{B}_0^T\mathbf{S}_0^T + \overline{\mathbf{L}}_{1m_f}\ .
\end{aligned} \tag{C.11}$$

Then take the transpose of the equations, corresponding to the powers z^0 to z^{-m_f} from (C.10):

$$\begin{aligned}
z^0 :\ & \mathbf{0} &&= -\Psi^T\mathbf{S}_0^T + \overline{\mathbf{B}}_0\overline{\mathbf{L}}_{10} + \overline{\mathbf{B}}_1\overline{\mathbf{L}}_{11} + \ldots + \overline{\mathbf{B}}_{m_f}\overline{\mathbf{L}}_{1m_f}\\
z^{-1} :\ & \mathbf{0} &&= -\Psi^T\mathbf{S}_1^T + \overline{\mathbf{B}}_0\overline{\mathbf{L}}_{11} + \overline{\mathbf{B}}_1\overline{\mathbf{L}}_{12} + \ldots + \overline{\mathbf{B}}_{m_f-1}\overline{\mathbf{L}}_{1m_f}\\
\vdots\ :\ & \vdots && \qquad\vdots\\
z^{-m_f+1} :\ & \mathbf{0} &&= -\Psi^T\mathbf{S}_{m_f-1}^T + \overline{\mathbf{B}}_0\overline{\mathbf{L}}_{1(m_f-1)} + \overline{\mathbf{B}}_1\overline{\mathbf{L}}_{1m_f}\\
z^{-m_f} :\ & \mathbf{0} &&= -\Psi^T\mathbf{S}_{m_f}^T + \overline{\mathbf{B}}_0\overline{\mathbf{L}}_{1m_f}.
\end{aligned} \tag{C.12}$$

Equations (C.11) and (C.12) contain $2(m_f+1)$ matrix equations and $2(m_f+1)$ unknown matrices. Bring them together into a system of linear equations, which yields

$$\left(\begin{array}{cccc|cccc}
\mathbf{B}_0^T & \mathbf{0} & \ldots & \mathbf{0} & \mathbf{I}_{n_d} & \mathbf{0} & \ldots & \mathbf{0}\\
\mathbf{B}_1^T & \mathbf{B}_0^T & \ldots & \mathbf{0} & \mathbf{0} & \mathbf{I}_{n_d} & \ddots & \mathbf{0}\\
\mathbf{B}_2^T & \mathbf{B}_1^T & \ddots & \mathbf{0} & \mathbf{0} & \ddots & \ddots & \mathbf{0}\\
\vdots & \vdots & \ddots & \vdots & \vdots & \vdots & \ddots & \vdots\\
\mathbf{B}_{m_f}^T & \mathbf{B}_{m_f-1}^T & \ldots & \mathbf{B}_0^T & \mathbf{0} & \mathbf{0} & \ldots & \mathbf{I}_{n_d}\\
\hline
-\Psi^T & \mathbf{0} & \ldots & \mathbf{0} & \bar{\mathbf{B}}_0 & \bar{\mathbf{B}}_1 & \ldots & \bar{\mathbf{B}}_{m_f}\\
\mathbf{0} & -\Psi^T & \ldots & \mathbf{0} & \mathbf{0} & \bar{\mathbf{B}}_0 & \ldots & \bar{\mathbf{B}}_{m_f-1}\\
\vdots & \vdots & \ddots & \vdots & \vdots & \vdots & \ddots & \vdots\\
\mathbf{0} & \mathbf{0} & \ldots & -\Psi^T & \mathbf{0} & \mathbf{0} & \ldots & \bar{\mathbf{B}}_0
\end{array}\right)
\left(\begin{array}{c}
\mathbf{S}_0^T\\ \mathbf{S}_1^T\\ \mathbf{S}_2^T\\ \vdots\\ \mathbf{S}_{m_f}^T\\ \hline \bar{\mathbf{L}}_{1m_f}\\ \bar{\mathbf{L}}_{1m_f-1}\\ \ldots\\ \bar{\mathbf{L}}_{10}
\end{array}\right)
=
\left(\begin{array}{c}
\mathbf{0}\\ \mathbf{0}\\ \vdots\\ \mathbf{0}\\ \mathbf{I}_{n_d}\\ \hline \mathbf{0}\\ \vdots\\ \mathbf{0}
\end{array}\right) \tag{C.13}$$

which is (4.25).

This system is solved with respect to the matrix coefficients $\mathbf{S}_i$ and $\mathbf{L}_{1i}$.

Notice that the system (C.13) has $(n_y + n_d)(m_f + 1)$ equations and an equal number of unknowns. As long as there is noise in the system, the system is solvable. However, when Ψ looses rank, the system can not always be guaranteed to have a unique solution for all combinations of n_y and n_d.

When (C.13) has been solved, the equations corresponding to powers of z from -1 to -n of (C.9) are used to calculate the coefficients of $\boldsymbol{Q}(z^{-1})$:

$$\begin{array}{rcl}
z^{-1}: & \mathbf{Q}_0 & = \mathbf{S}_{m_f}\mathbf{B}_1 + \mathbf{S}_{m_f-1}\mathbf{B}_2 + \ldots + \mathbf{S}_1\mathbf{B}_{m_f} + \mathbf{S}_0\mathbf{B}_{m_f+1} \\
z^{-2}: & \mathbf{Q}_1 & = \mathbf{S}_{m_f}\mathbf{B}_2 + \mathbf{S}_{m_f-1}\mathbf{B}_3 + \ldots + \mathbf{S}_1\mathbf{B}_{m_f+1} + \mathbf{S}_0\mathbf{B}_{m_f+2} \\
\vdots: & \vdots & \vdots \qquad\qquad\qquad\qquad \vdots \\
z^{-n-m_f}: & \mathbf{Q}_{n-m_f-1} & = \mathbf{S}_{m_f}\mathbf{B}_{n-m_f} + \mathbf{S}_{m_f-1}\mathbf{B}_{n-m_f+1} + \ldots + \mathbf{S}_1\mathbf{B}_{n-1} + \mathbf{S}_0\mathbf{B}_n \\
z^{-n-m_f-1}: & \mathbf{Q}_{n-m_f-2} & = \mathbf{S}_{m_f}\mathbf{B}_{n-m_f+1} + \mathbf{S}_{m_f-1}\mathbf{B}_{n-m_f+2} + \ldots + \mathbf{S}_1\mathbf{B}_n \\
\vdots: & \vdots & \vdots \qquad\qquad\qquad\qquad \vdots \\
z^{-n+1}: & \mathbf{Q}_{n-2} & = \mathbf{S}_{m_f}\mathbf{B}_{n-1} + \mathbf{S}_{m_f-1}\mathbf{B}_n \\
z^{-n}: & \mathbf{Q}_{n-1} & = \mathbf{S}_{m_f}\mathbf{B}_n \ .
\end{array} \qquad \text{(C.14)}$$

Bringing (C.14) into matrix form results in (4.26). The matrix polynomial $\boldsymbol{L}_2(z^{-1})$ can be calculated in a similar way as $\boldsymbol{Q}(z^{-1})$ was calculated, but this polynomial is not needed. As always, if $m_f > n$, the additional channel taps are simply set to zero in the equations above.

Equations (C.11), (C.12) and (C.14) are the equations needed to calculate the multivariable DFE.